One-Dimensional Periodic Leaky-Wave Antennas

Paolo Baccarelli

"La Sapienza" University of Rome

Electronic Engineering Department

Outline

- Generalities of One-Dimensional (1D) Periodic Structures
- Axially Periodic 2D Structure: A Metal Strip Grating on a Grounded Dielectric Slab (MSG-GDS)
- Design of 1D Periodic Leaky-Wave Antenna: A Printed Leaky-Wave 'Bull-Eye' Antenna with Suppressed Surface-Wave
- Axially Periodic 3D Structure: A Periodically Loaded Microstrip Line

Geometry: Axially Periodic 2D Structures

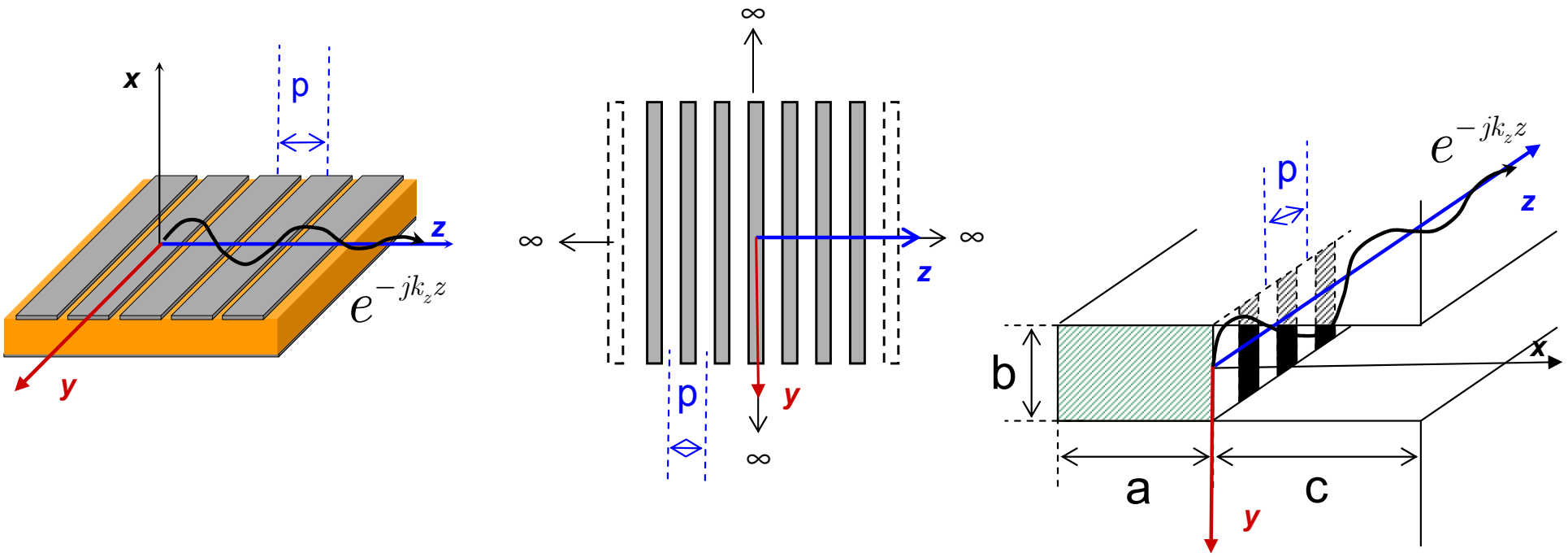

1D periodic structure: ***Translational symmetry*** along the direction ***z***, infinitely extended domain of **periodicity** along *z* with spatial period equal to ***p***

Axially periodic structure: Propagation of Guided and Leaky Modes along the direction of periodicity z

2D Structure: Absence of *y* variation in the structure and in the field [$\partial(\ )/\partial y=0$]

Geometry: Axially Periodic 3D Structures

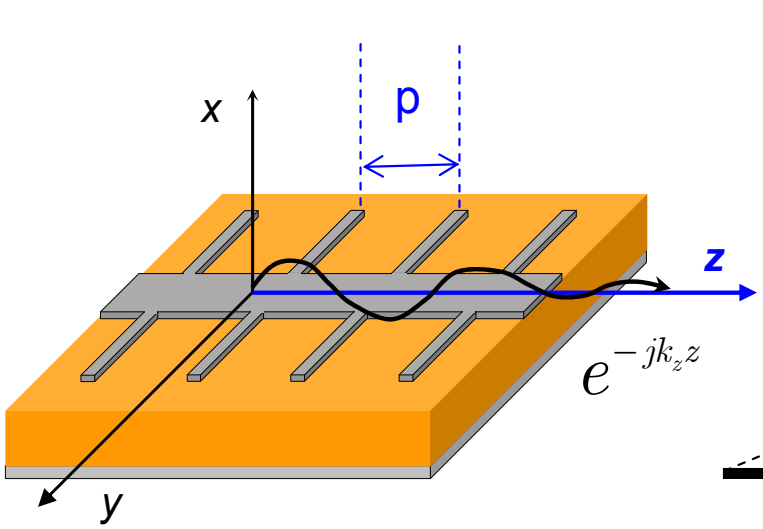

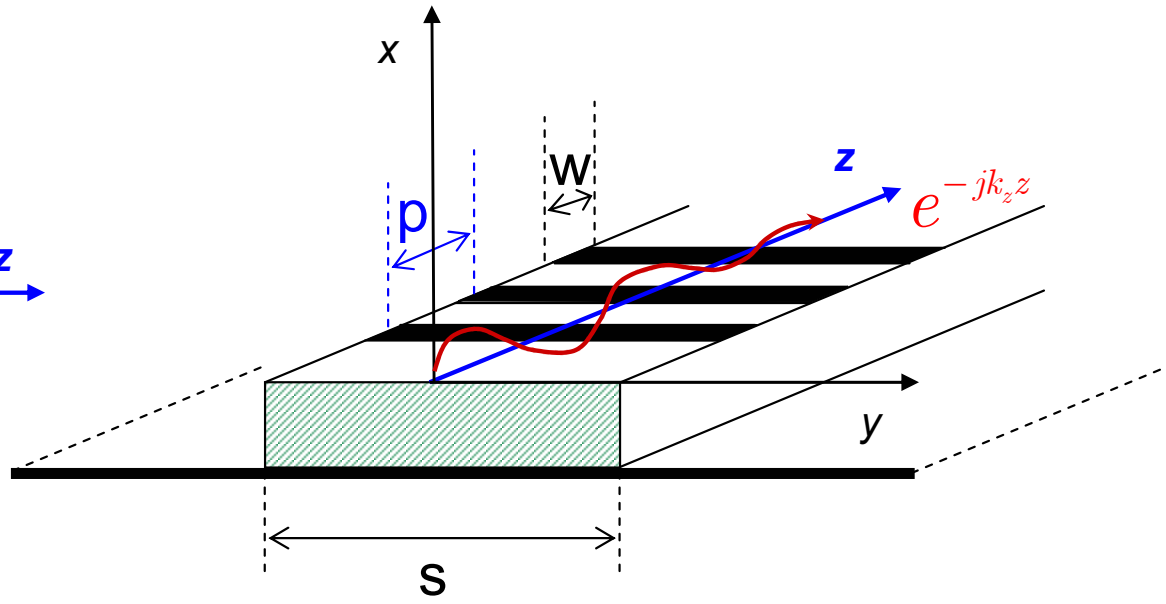

1D periodic structure: ***Translational symmetry*** along the direction ***z***, infinitely extended domain of **periodicity** along *z* with spatial period equal to ***p***

Axially periodic structure: Propagation of Guided and Leaky Modes along the direction of periodicity z

3D Structure: *General* transverse *variation* of the field [$\partial(\ )/\partial y \neq 0$]

Geometry: Linear (Phased) Arrays of Leaky-Wave Line Sources

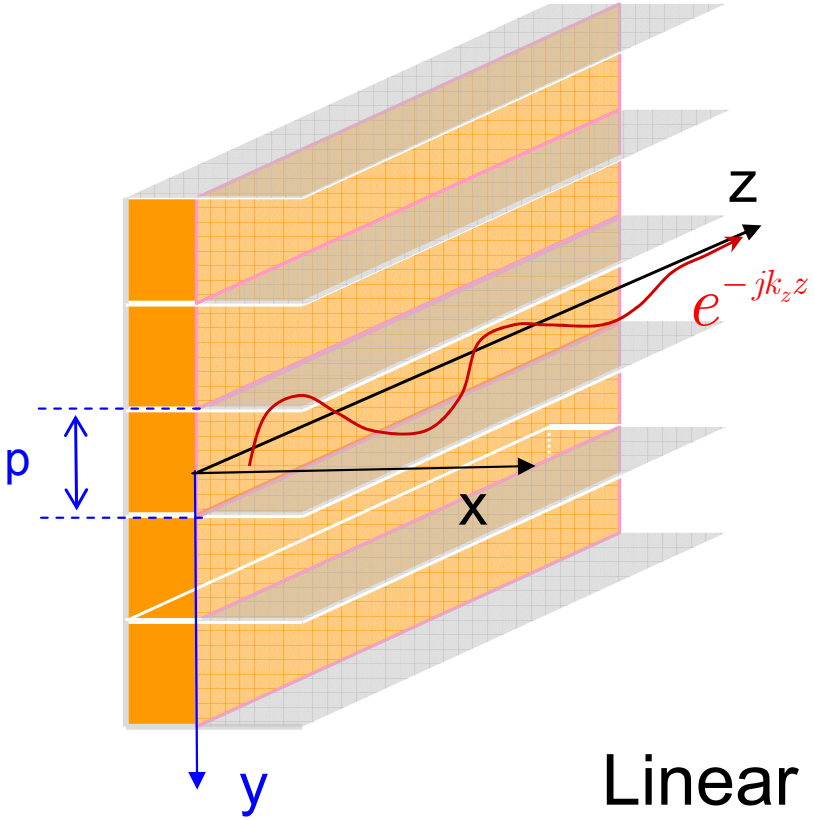

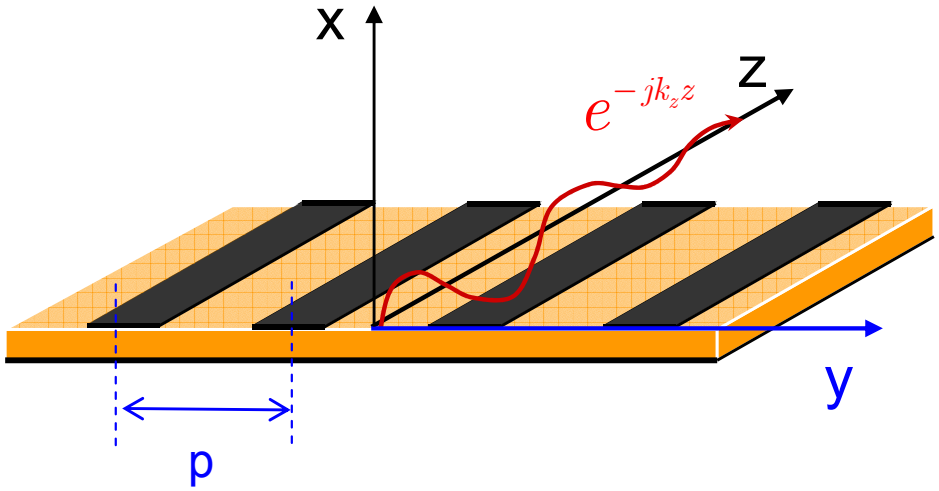

Linear Arrays

1D periodic structure: ***Translational symmetry*** along the direction ***y***, infinitely extended domain of **periodicity** along *y* with spatial period equal to ***p***

Leaky-Wave line source: Propagation of Guided and Leaky Modes along the infinite **uniform** direction z

General Radiative Properties

Axially
Periodic
2D&3D Structures

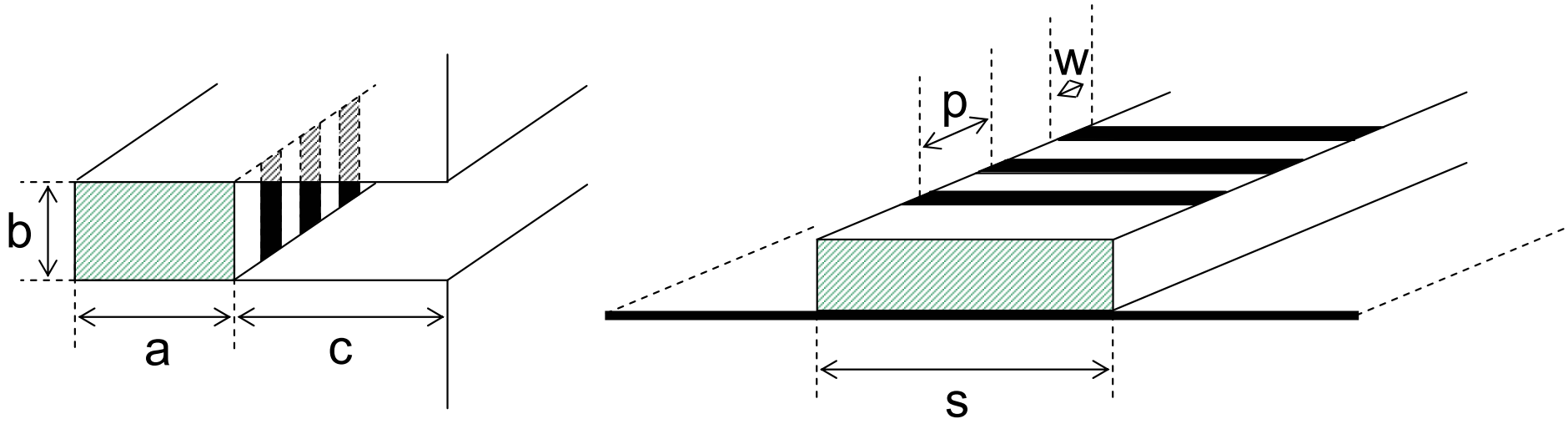

Periodic loading of a basically slow-wave open structure produces a fast complex (leaky) wave which continuously radiates power

1. Very low attenuation rate and large effective aperture: High Directivity
2. Various degrees of freedom in control of aperture distribution: Pattern Shaping
3. Backward and forward leakage regimes: Wide-Angular Beam Scanning

Characteristic Features of Traveling Waves

Axially Periodic 2D&3D Structures

$p/\lambda_0 << 1$

Basically slow, periodic loaded structures
in general support ***bound modes*** or ***surface waves***.
Radiation in the forward quadrant is in some cases permitted.
Recently proposed quasi-uniform periodic structures (***Metamaterials***)
have revealed scanning capability in both the forward and backward quadrants

$p/\lambda_0 > 1/2$

When *p* is sufficiently large, a **fast complex** (leaky) **wave** appears,
which gives rise to radiation at some angle between backfire and endfire

Mutual interaction of periodic elements is responsible for mode-coupling resonances,
thus affecting the formation of pass and stop bands, the operating bandwidth,
as well as the radiation properties and scan angles.

Appropriate analysis of EM fields
and accurate description of guided and leaky modes
in axially periodic 2D and 3D structures

Floquet's Theorem

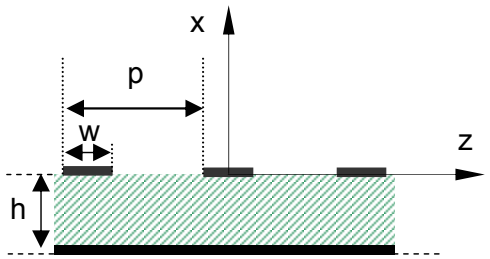

A time-harmonic ($e^{j\omega t}$) electromagnetic field $\mathbf{E}(x,z)$ of a normal mode guided along an ***axially periodic 2D structure*** [absence of *y* variation, [$\partial(\ )/\partial y=0$] possesses the property:

$$\mathbf{E}\left(x,z+p\right)=e^{-jk_{z0}p}\,\mathbf{E}\left(x,z\right)$$

$k_{z0}=\beta_0-j\alpha$ Generally complex fundamental propagation constant k_{z0}: β_0 and α are the corresponding phase and attenuation constants

Bloch-Wave Form:

$$\mathbf{E}\left(x,z\right)=e^{-jk_{z0}z}\,\mathbf{P}(x,z)$$

$$\mathbf{P}(x,z+p)=\mathbf{P}(x,z)$$

Unique determination of the guided-wave field at any point on an infinite periodic structure solely from the knowledge of the field distribution within the **Unit Cell** (i.e., a *single period* of width ***p***)

Spatial Harmonic Expansion

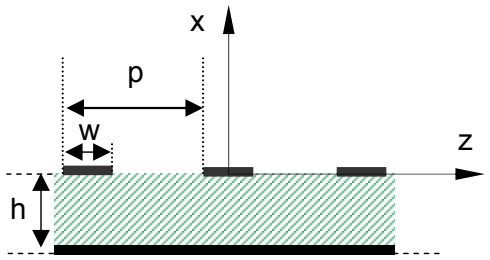

The periodic vector function $\mathbf{P}(x+p,z) = \mathbf{P}(x,z)$ may be expanded in a Fourier series

$$\mathbf{P}(x,z) = \sum_{n=-\infty}^{+\infty} \mathbf{a}_n(x) e^{-jn2\pi z/p}$$

$$\mathbf{E}(x,z) = \sum_{n=-\infty}^{+\infty} \mathbf{a}_n(x) e^{-jk_{zn}z}$$

The Fourier series expansion of a Bloch Wave indicates that the field of a normal mode is expressible in terms of an ***infinite number*** of ***traveling waves***, called ***spatial harmonics***

$$k_{zn} = \beta_n - j\alpha,$$
$$\beta_n = \beta_0 + n2\pi/p\ ,$$
$$n = 0, \pm 1, \pm 2, \ldots$$

The wavenumbers k_{zn} represent the spatial harmonic axial *propagation constants*, with different *phase* constants β_n and the same *attenuation* constant α

$\mathbf{a}_n(x)$ Spatial harmonic complex amplitudes

General Properties of the Spatial Harmonic Expansion

$$\mathbf{E}(x,z) = \sum_{n=-\infty}^{+\infty} \mathbf{a}_n(x) e^{-jk_{zn}z}$$

$|\mathbf{a}_n(x)| \to 0$, as $|n| \to \infty$ → Very often a ***single*** dominant n=0 spatial harmonic describes the field adequately. However, during *mode coupling resonances* ***more*** spatial harmonics are required

A ***single*** spatial harmonic does ***not*** satisfy ***boundary conditions*** → A normal ***mode*** of the periodic structure is represented by the ***entire*** spatial harmonic expansion

The spatial harmonics also represent axially traveling waves along z, with *uniform amplitude* for *real values* of k_{z0} → The ***spatial harmonic expansion*** constitutes a ***field representation*** alternative to that in terms of *ordinary waveguide modes*

General Properties of the Spatial Harmonic Expansion

$$\mathbf{E}(x,z) = \sum_{n=-\infty}^{+\infty} \mathbf{a}_n(x) e^{-jk_{zn}z}$$

Each spatial harmonic possesses a ***different*** axial phase velocity:

$$u_{zn} = \frac{\omega}{\beta_{zn}} = \frac{\omega}{\beta_{z0} + n2\pi/p}$$

→ For ***high*** values of |n| all spatial harmonics are axially ***slow*** waves. For $\beta_0 \geq 0$, the $n > 0$ are ***forward***-traveling, all those with $\beta_n < 0$ are ***backward***-traveling.

Each spatial harmonic possesses the **same** group velocity of the normal mode:

$$v_{gn} = \frac{d\omega}{d\beta_{zn}} = \frac{d\omega}{d\beta_{z0}} = v_g$$

→ Each spatial harmonic carries power in the direction of periodicity. However, the total axial power flow is **not** a **sum** of axial powers carried by the individual space harmonics.

$$\mathbf{a}_n(x) = \mathbf{a}_n e^{-jk_{xn}x}$$

$$k_{xn} = \sqrt{k_0^2 - k_{zn}^2}$$

$$n = 0, \pm 1, \pm 2, \ldots$$

$$k_0 = \omega\sqrt{\mu_0 \varepsilon_0}$$

→ In the exterior region, the field of each spatial harmonic constitutes a homogeneous or inhomogeneous plane wave. Each spatial harmonic ***may independently radiate*** in free space.

Modal Analysis of Axially Periodic 2D Structures

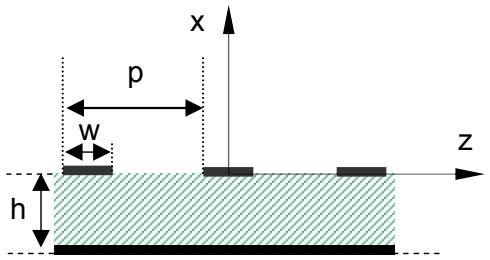

Dispersion relation of an axially periodic, traveling-wave structure

$$\mathrm{D}\left(k_{z0}, k_0\right) = 0 \quad \longrightarrow \quad \boxed{k_{z0} = k_{z0}\left(k_0\right)}$$

Fundamental propagation constant of a normal mode as function of frequency

$$k_{zn} = k_{z0} + n2\pi/p = \beta_0 + n2\pi/p - j\alpha$$

All spatial harmonic wave numbers ***must be solutions*** of the ***same*** dispersion equation

The **classification** of **guided-wave types** on these structures is based on the traveling-wave properties of ***each*** spatial harmonic in the ***exterior region*** (*free space*)

$$\mathbf{E}\left(x,z\right) = \sum_{n=-\infty}^{+\infty} \mathbf{a}_n \, e^{-jk_{xn}x} \, e^{-jk_{zn}z}$$

$$k_{xn} = \sqrt{k_0^2 - k_{zn}^2} \cong -j\alpha_{xn}$$

Slow-Wave Type (***Bound***)

$$k_{xn} = \sqrt{k_0^2 - k_{zn}^2} \cong \beta_{xn}$$

Fast-Wave Type (***Radiative***)

Brillouin Diagram

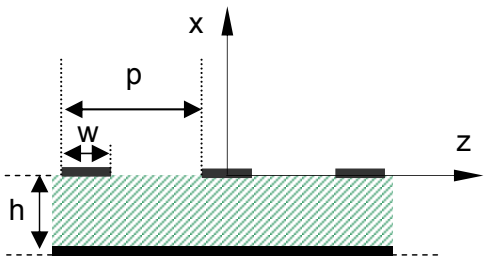

The ***Brillouin Diagram*** gives most of the ***properties*** of ***open*** axially periodic structure: it is a ***graphic representation*** of the ***dispersion relation*** of the space-harmonic axial phase constants

$$\beta_n = \beta_0 + n\,2\pi/p,$$
$$n = 0, \pm 1, \pm 2, \ldots$$

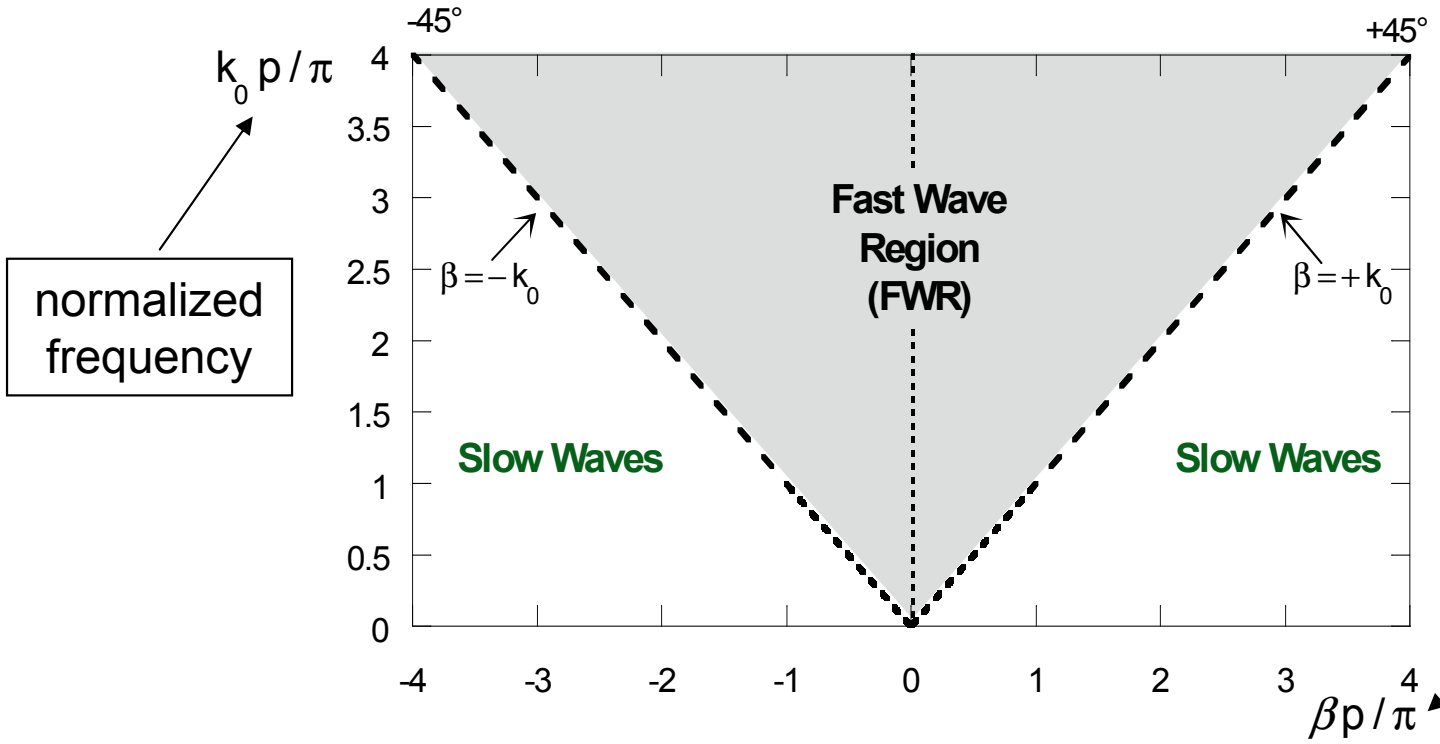

normalized frequency

normalized phase constant

FWR:

$$|\beta_n| < k_0,$$
$$n = 0, \pm 1, \pm 2, \ldots$$

Brillouin Diagram

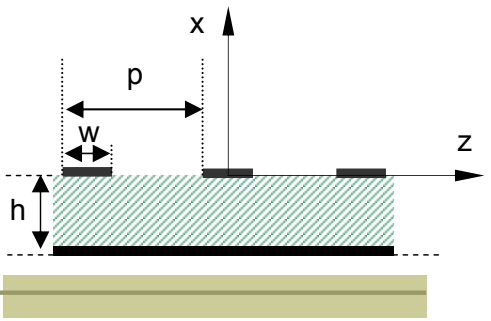

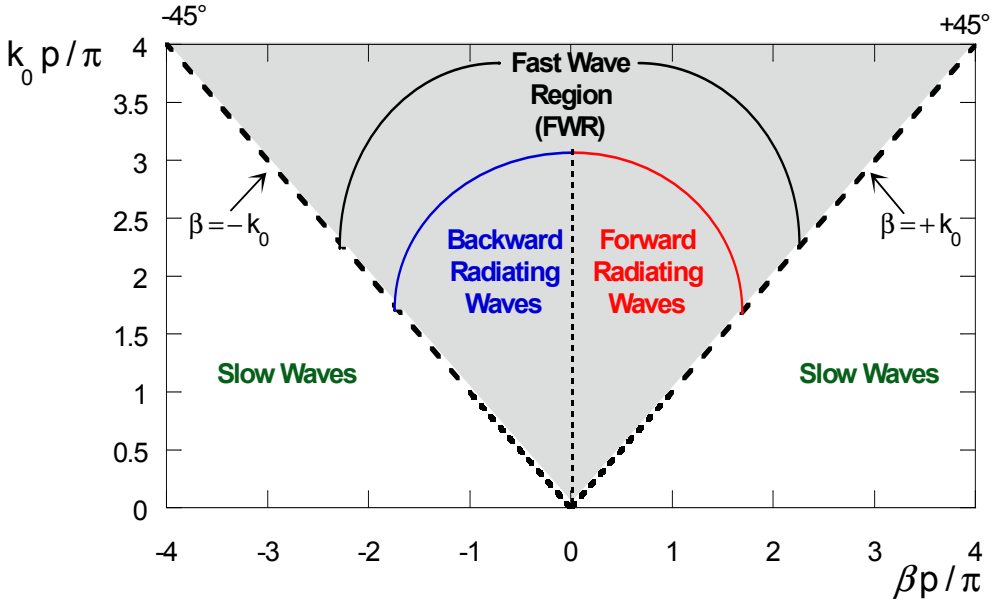

The n^{th} spatial harmonic is axially ***slow*** only if the corresponding point ($\beta_n p/\pi, k_0 p/\pi$) of the dispersion curve is located <u>*outside*</u> the ***FWR***

$$k_{zn} = \beta_n - j\alpha \quad \text{or} \quad k_{zn} = \beta_n$$
$$|\beta_n| = |\beta_0 + n\,2\pi/p| > k_0$$
$$k_{xn} = \sqrt{k_0^2 - k_{zn}^2} \cong -j\alpha_{xn}$$

The n^{th} spatial harmonic is axially ***fast*** only if the corresponding point ($\beta_n p/\pi, k_0 p/\pi$) of the dispersion curve is located <u>*inside*</u> the ***FWR***

$$k_{zn} = \beta_n - j\alpha$$
$$|\beta_n| = |\beta_0 + n\,2\pi/p| < k_0$$
$$k_{xn} = \sqrt{k_0^2 - k_{zn}^2} \cong \beta_{xn}$$

Backward-Radiating Wave

$$-k_0 < \beta_n < 0$$

Forward-Radiating Wave

$$0 < \beta_n < k_0$$

Brillouin Diagram

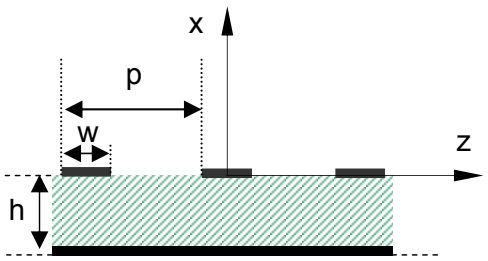

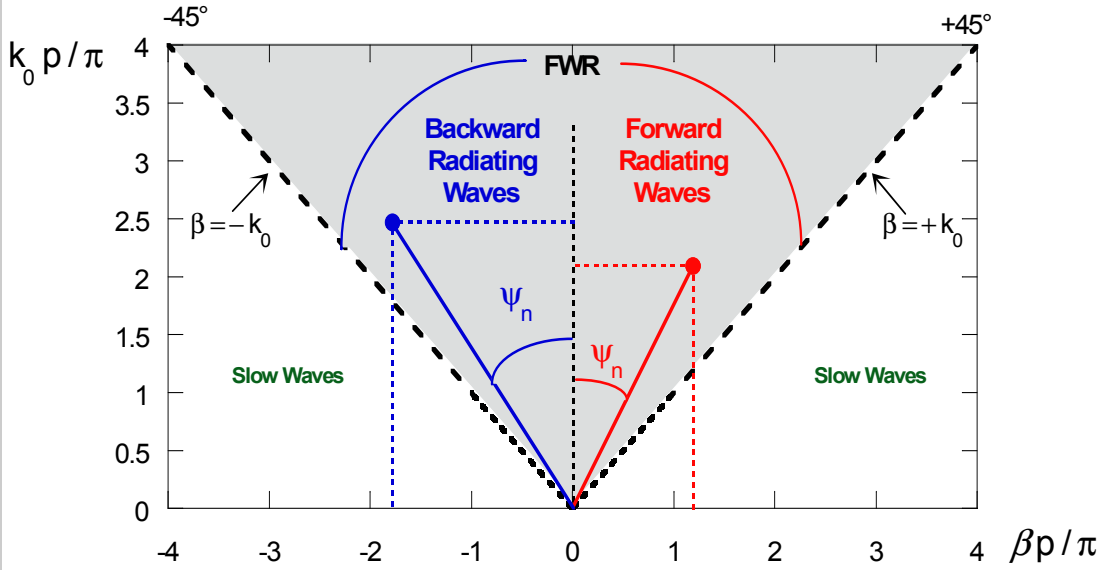

The Brillouin diagram permits a rapid determination, as a function of the normalized frequency, of the ***number*** of radiating beams and of their respective ***angles of radiation***

For the nth radiating harmonic the relation between the peak of the radiation lobe measured from broadside θ_n and its angle ψ_n with respect to the $k_0 p/\pi$ axis in the Brillouin diagram is:

$$\sin\theta_n = \frac{\beta_0 + n\,2\pi/p}{k_0} = \frac{\beta_0 p/\pi + 2n}{k_0 p/\pi} = \tan\psi_n$$

$-k_0 < \beta_0 + n\,2\pi/p < 0$ $\quad$ $\psi_n < 0$ $\quad$ $\theta_n < 0$

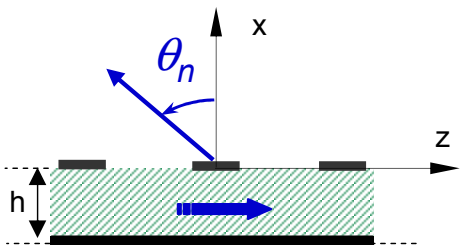

Backward-Radiating Wave

$0 < \beta_0 + n\,2\pi/p < k_0$ $\quad$ $\psi_n > 0$ $\quad$ $\theta_n > 0$

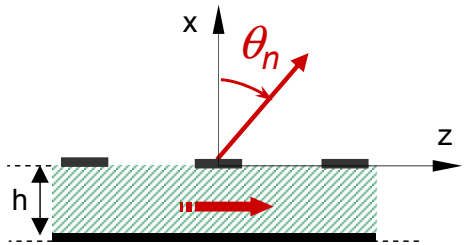

Forward-Radiating Wave

Brillouin Diagram: Closed 1D Periodic TEM Structures

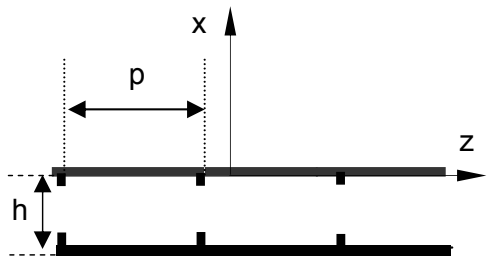

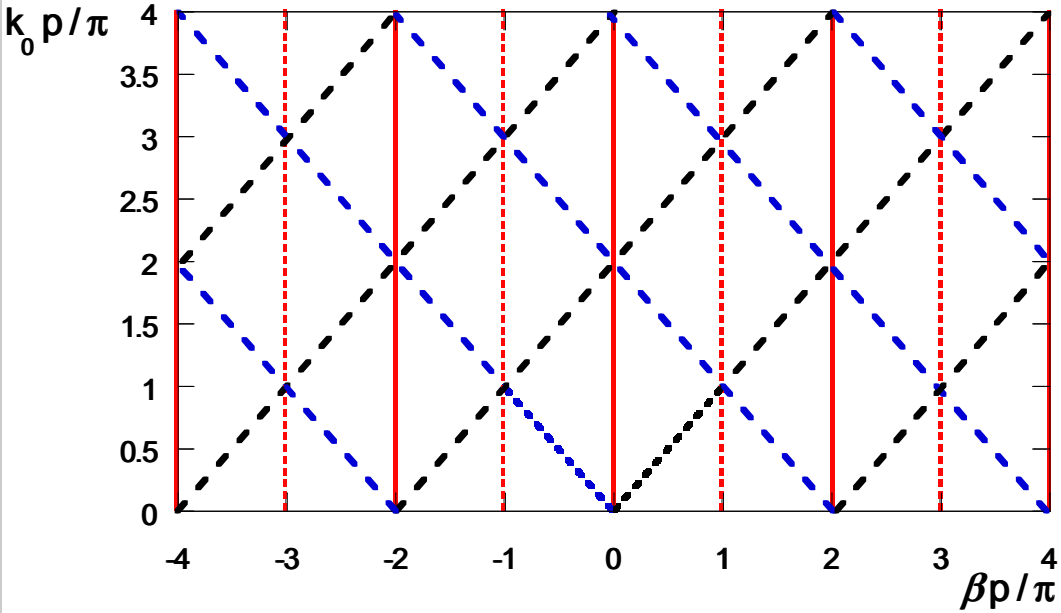

In the limit of ***Vanishing Loading***

$$\beta_n = \beta_0 + n\,2\pi/p,$$

$$\beta_0 = \omega\sqrt{\mu\varepsilon}$$

$$n = 0, \pm 1, \pm 2, \ldots$$

Brillouin Diagram of an axially periodic structure ***repeats*** in $\beta p/\pi$ with ***period*** $2p/\pi$

The dispersion relation of the spatial harmonics ***repeat*** with a translation equal to $2n$ parallel to the abscissa axis

If the periodic structure is ***reciprocal*** ($\beta_0 \leftrightarrow -\beta_0$) the Brillouin diagram is ***symmetric*** with respect to the ***ordinate axis***

The Brillouin diagram is **symmetric** with respect to the **axes**:

$$\beta_n p/\pi = n,\ n = 0, \pm 1, \pm 2, \ldots$$

Brillouin Diagram: Radiation Regions in Open 2D Structures

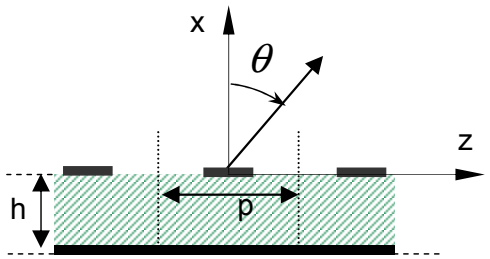

In the limit of vanishing loading

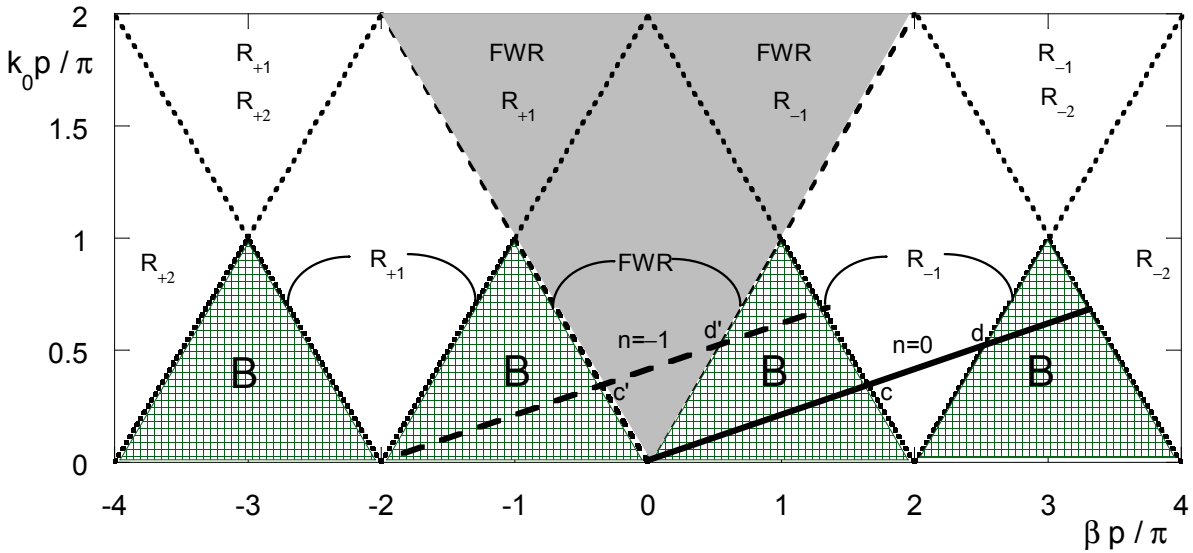

Superposition of an infinite number of identical (k_0p/π, $\beta_n p/\pi$) planes, one for each n, which individually possess their own FWR

The ***Radiation Region*** $\mathbf{R}_n$ of the n^{th} harmonic is the set of points (k_0p/π, β_0p/π) of the n=0 harmonic, corresponding to which the n^{th} harmonic is located in the FWR

$$\mathrm{R}_n:\ \left(k_0 p\right)^2-\left(\beta_0 p+2\pi n\right)^2\geq 0,\quad n=0,\pm1,\pm2,\ldots$$

All spatial harmonics are ***simultaneously slow*** in the shaded triangular regions with $\mathbf{k_0p < \pi}$, which are termed the ***Bound-Wave Regions*** (**B**)

Brillouin Diagram: Mode Coupling in Open 2D Structures

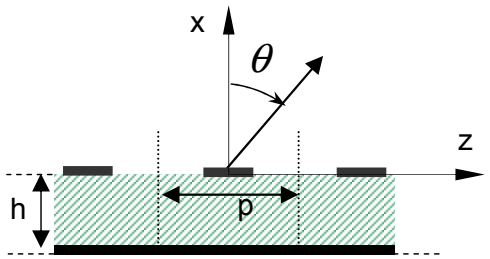

Mutual interactions between (different) backward ($v_g<0$) - and forward ($v_g>0$) - traveling space harmonics give rise to ***Mode Coupling***:
Contra-Directional Coupling at $\beta p/\pi = n$, **n=0,±1, ± 2,..**

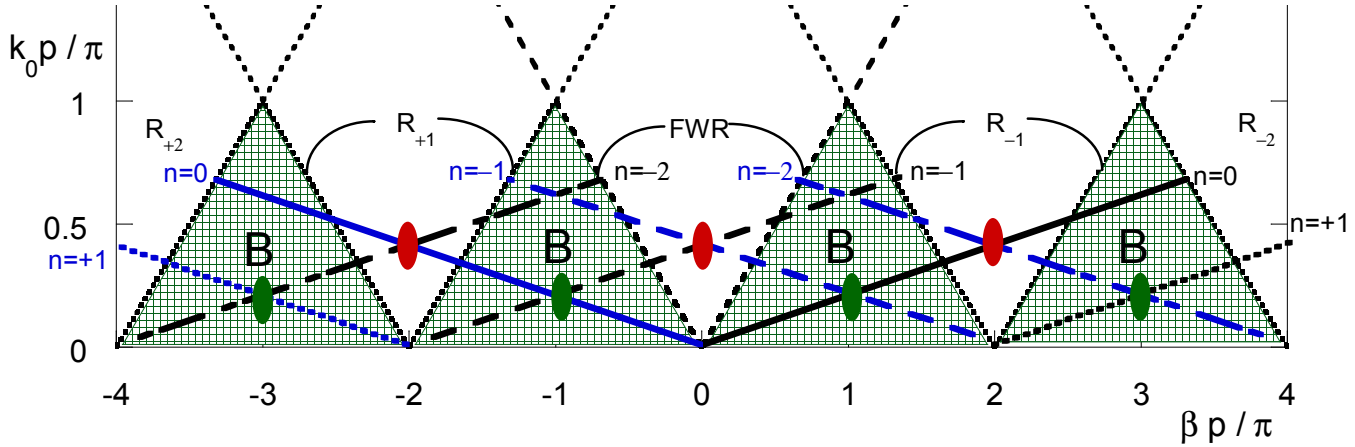

- ***Closed Stop Band***: The entire modal field is bounded and highly attenuated ($\alpha/k_0>>0$), the interaction between harmonics forms a standing wave along z

- ***Open Stop Band***: Coupling between two spatial harmonics radiating at broadside; high degradation of the radiation properties at broadside.

Spectral Properties of Spatial Harmonics

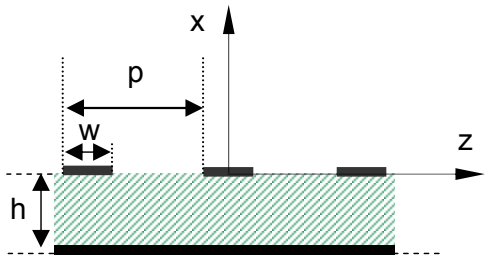

The ***Dispersion Relation*** of an ***open*** axially periodic traveling-wave structure is an ***odd*** function of k_{xn}, for n=0,±1, ± 2,…; the overall Riemann Surface of D(k_{z0},k_0) consists of a denumerably ***infinite number*** of sheets

$$k_{xn}^2 = |k_{xn}|^2 e^{-j\phi} = k_0^2 - k_{zn}^2 ,$$

$$k_{xn} = |k_{xn}| e^{-j\phi/2} = \sqrt{k_0^2 - k_{zn}^2} = \beta_{xn} - j\alpha_{xn} ,$$

$$n = 0, \pm 1, \pm 2, \ldots$$

$$\begin{cases} 0 \le \phi < 2\pi \\ \Im\mathrm{m}\left(k_{xn}\right) < 0 \\ \alpha_{xn} > 0 \end{cases}$$

Top Sheet of k_{xn}^2: Proper Determination

$$\begin{cases} 2\pi \le \phi < 4\pi \\ \Im\mathrm{m}\left(k_{xn}\right) > 0 \\ \alpha_{xn} < 0 \end{cases}$$

Bottom Sheet of k_{xn}^2: Improper Determination

$$\mathbf{E}(x,z) = \sum_{n=-\infty}^{+\infty} \mathbf{a}_n e^{-jk_{xn}x} e^{-jk_{zn}z}$$

A guided Bloch Wave is a superposition of various proper and improper spatial harmonics

A ***proper surface wave*** **E**(*x*,*z*) is characterized by a *real value* of k_{z0} and **all** axially slow **proper** spatial harmonics

For *complex values* of k_{z0}, **E**(*x*,*z*) is called a ***proper complex*** Bloch Wave when **all** spatial harmonics are **proper**, and is otherwise termed **improper**

Spectral Properties of Spatial Harmonics

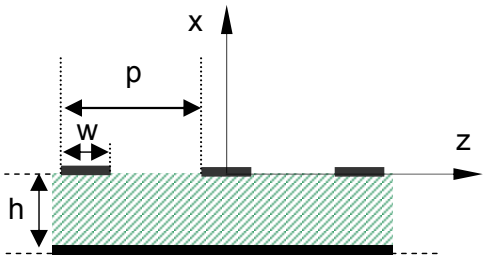

$$k_{xn}^2 = k_0^2 - \beta_n^2 + \alpha^2 + j2\beta_n\alpha$$

$0 \le \phi < 2\pi$

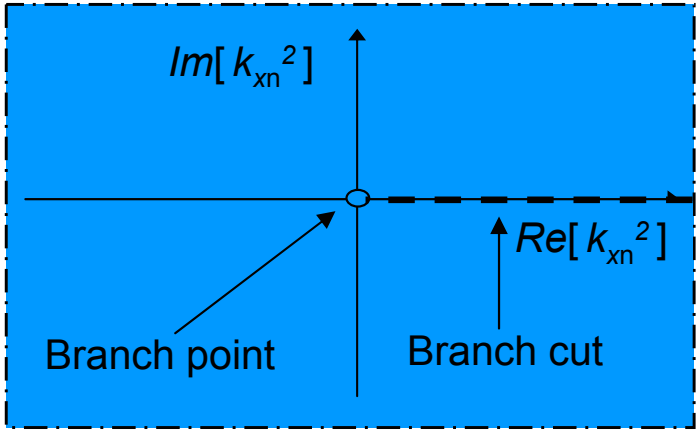

$\Im\mathrm{m}\left(k_{xn}\right) < 0$

$2\pi \le \phi < 4\pi$

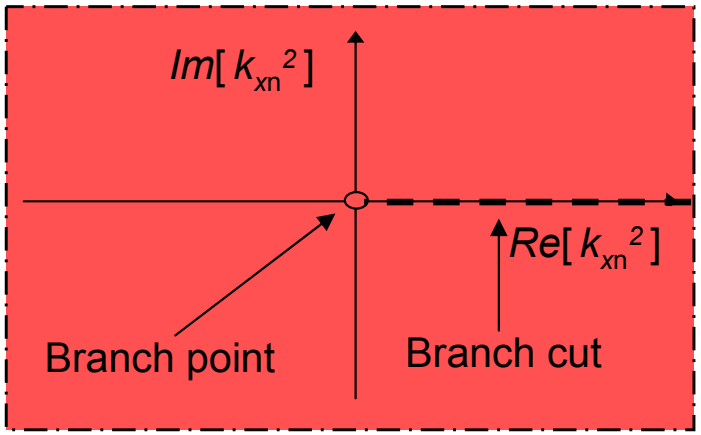

$\Im\mathrm{m}\left(k_{xn}\right) > 0$

k_{xn}^2 may change sheets only when either the **branch cut** or the **branch point** $k_{xn}=0$ is ***crossed***

$$\begin{cases} \Re\mathrm{e}\left(k_{xn}^2\right) \ge 0 \\ \Im\mathrm{m}\left(k_{xn}^2\right) > 0 \leftrightarrow \Im m\left(k_{xn}^2\right) < 0 \end{cases}$$

$$\beta_0 = -\frac{2\pi n}{p} \quad \textbf{or} \quad \begin{cases} \beta_n^2 < k_0^2 \\ \alpha = 0 \end{cases}$$

branch cut crossing

$$\begin{cases} \beta_n = \pm k_0 \\ \alpha = 0 \end{cases}$$

branch point crossing

Brillouin Diagram and Spectral Properties of Spatial Harmonics

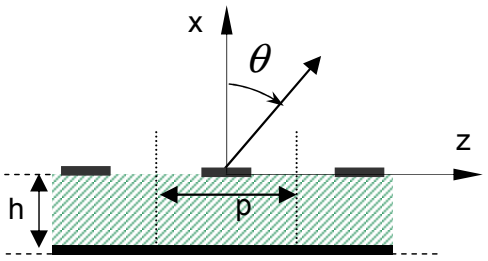

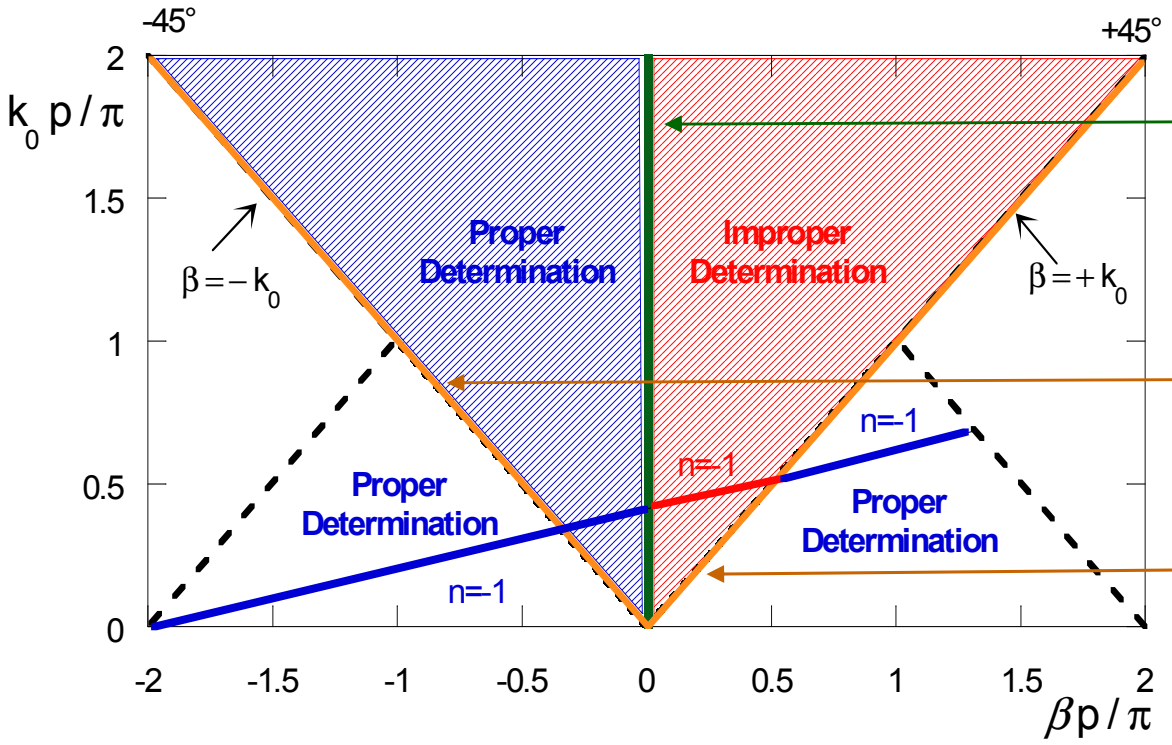

$$\beta_0 = -\frac{2\pi n}{p}$$

branch cut crossing

$$\begin{cases} \beta_n = \pm k_0 \\ \alpha = 0 \end{cases}$$

branch point crossing

A Backward-Radiating spatial harmonic is **proper** and its field **decays away** from the structure:
Backward-Leaky Waves

A Forward-Radiating spatial harmonic is **improper** and its field **grows** at infinity along *x* :
Forward-Leaky Waves

A Canonical Axially Periodic 2D Structure: Metal-Strip Grating on a Grounded Dielectric Slab

- ***Translational symmetry*** of an axially periodic structure: Infinitely extended domain along the ***axial*** direction of periodicity *z*, with spatial period equal to ***p***
- **2D Structure**: Absence of *y* variation in the structure and in the field [$\partial(\ )/\partial y=0$]
- Metal-Strip Grating on a Grounded Dielectric Slab (MSG-GDS): ***modal analysis*** along the axial direction of periodicity *z*

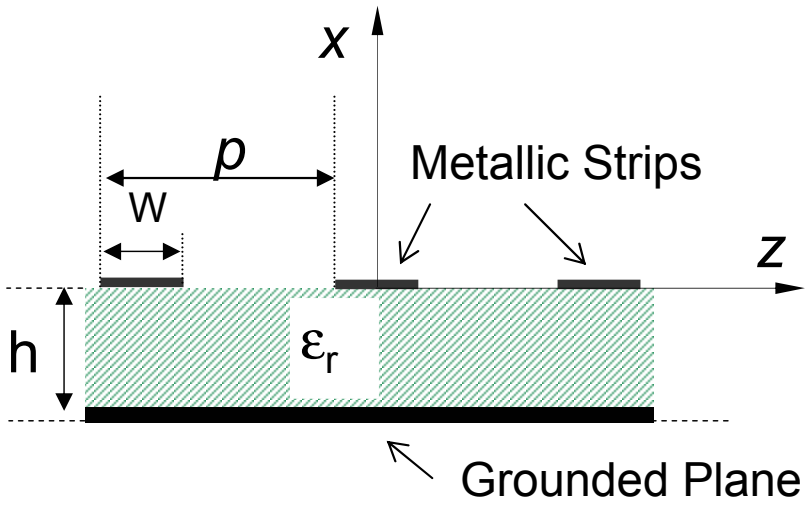

MSG-GDS: Spectral Representation of 1D Periodic Currents

Spatial periodicity of the currents on metal strips along *z*

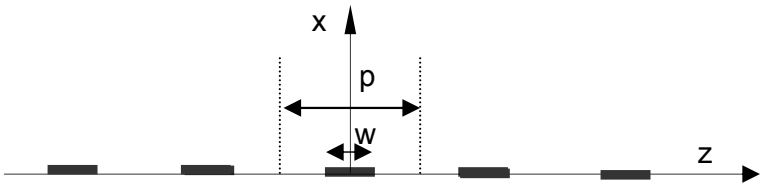

Discrete spectrum of the spectral currents as function of the variable k_z, $\Delta k_z \rightarrow n\,2\pi/p$

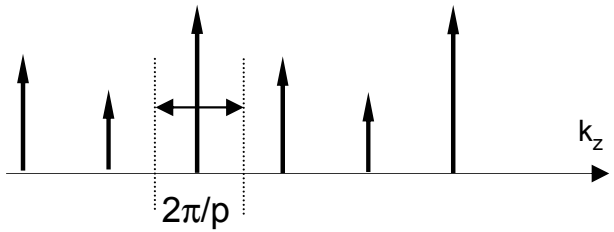

$$\mathbf{J}_s^p(z) = \sum_{n=-\infty}^{+\infty} \tilde{\mathbf{J}}_{sn} e^{-jk_{zn}z} \quad \Longleftrightarrow \quad \tilde{\mathbf{J}}_s^p(k_z) = \sum_{n=-\infty}^{+\infty} \tilde{\mathbf{J}}_{sn}\,\delta\left(k_z - k_{zn}\right)$$

$$\int_{-p/2}^{p/2} \mathbf{J}_s^p(z) e^{jk_{zm}z} dz = \sum_{n=-\infty}^{+\infty} \tilde{\mathbf{J}}_{sn} \int_{-p/2}^{p/2} e^{-j(k_{zn}-k_{zm})z} dz$$

Fourier Transform of the current on the strip within the **Unit Cell**

$$\tilde{\mathbf{J}}_s^0(k_{zm}) = \int_{-\infty}^{+\infty} \mathbf{J}_s^0(z) e^{jk_{zm}z} dz$$

$$\tilde{\mathbf{J}}_{sn} = \frac{1}{p}\tilde{\mathbf{J}}_s^0(k_{zn})$$

Orthogonality relations for Spatial Harmonics

$$\int_{-p/2}^{p/2} e^{-j(k_{zn}-k_{zm})z} dz = \begin{cases} 0, & m \neq n \\ p, & m = n \end{cases}$$

MSG-GDS: Integral Equation within the Unit Cell

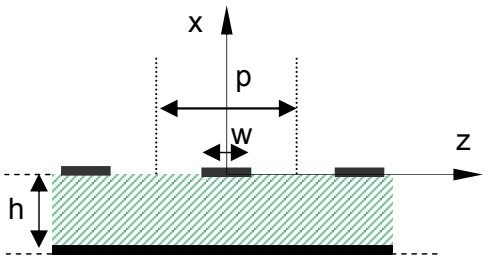

Space Domain

$$\mathbf{E}(x,z)=\int_{-\infty}^{+\infty}\overline{\mathbf{G}}_{ee}(x,0;z-z')\cdot\mathbf{J}_s(z')dz'$$

Spectral Domain k_z

$$\tilde{\mathbf{E}}(x;k_z)=\tilde{\mathbf{G}}_{ee}(x,0;k_z)\cdot\tilde{\mathbf{J}}_s(k_z)$$

Spatial harmonic **expansion** of the Electric Field

$$\mathbf{E}(x,z)=\frac{1}{2\pi p}\sum_{n=-\infty}^{+\infty}\tilde{\mathbf{G}}_{ee}(x,0;k_{zn})\cdot\tilde{\mathbf{J}}_s^0(k_{zn})e^{-jk_{zn}z}$$

$$\tilde{\mathbf{E}}(x;k_z)=\tilde{\mathbf{G}}_{ee}(x,0;k_z)\cdot\frac{1}{p}\sum_{n=-\infty}^{+\infty}\tilde{\mathbf{J}}_s^0\,\delta(k_z-k_{zn})$$

$$\hat{\mathbf{x}}\times\sum_{n=-\infty}^{+\infty}\tilde{\mathbf{G}}_{ee}(0,0;k_{zn})\cdot\tilde{\mathbf{J}}_s^0(k_{zn})e^{-jk_{zn}z}=\mathbf{0}\,,\quad |z|<w/2$$

Integral Equation obtained by enforcing that the tangential electric field **vanishes** on the strip within the ***Unit Cell***

MSG-GDS: Method of Moments Discretization of the Integral Equation

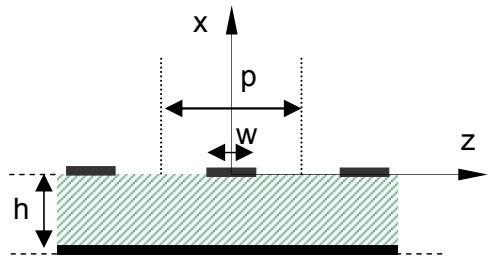

$$\mathbf{J}_s(z) = J_y(z)\hat{\mathbf{y}} + J_z(z)\hat{\mathbf{z}} \cong \sum_{r=0}^{N_y-1} A_r J_{yr}(z)\hat{\mathbf{y}} + \sum_{s=0}^{N_z-1} B_s J_{zr}(z)\hat{\mathbf{z}}$$

2D Structure

TE_z Modes — **TM_z Modes**

Representation of the transversal and longitudinal components of the unknown currents by means of an appropriate set of basis functions ***(Chebyshev polynomials)***

Testing of the Integral Equation within the ***Unit Cell***

$$\int_{-p/2}^{p/2} \left[J_{yl}(z)\hat{\mathbf{y}}\right] \cdot \sum_{r=0}^{N_y-1} A_r \sum_{n=-\infty}^{+\infty} \tilde{\mathbf{G}}_{ee}(0,0;k_{zn}) \cdot \left[\tilde{J}_{yr}(k_{zn})\hat{\mathbf{y}}\right] e^{-jk_{zn}z} dz = \mathbf{0}\,,$$

$$l = 0,..,N_y - 1 \qquad |z| < p/2$$

$$J_{yr}(z) = \frac{T_{2r}\left(\frac{2z}{w}\right)}{\sqrt{1-\left(\frac{2z}{w}\right)^2}}$$

$$J_{zs}(z) = jU_{2s-1}\left(\frac{2z}{w}\right)\sqrt{1-\left(\frac{2z}{w}\right)^2}$$

$$\sum_{r=0}^{N_y-1} A_r Z_{yy,lr}(k_{zn}, f) = 0\,, \quad l = 0,..,N_y - 1$$

$$Z_{yy,pr}(k_{zn}, f) = \sum_{n=-\infty}^{+\infty} \tilde{J}_{yp}(-k_{zn})\tilde{G}_{ee,yy}(0,0;k_{zn})\tilde{J}_{yr}(k_{zn})\,;\; p,r = 0,..,N_y - 1$$

MSG-GDS: Dispersion relation for TE_z and TM_z Modes

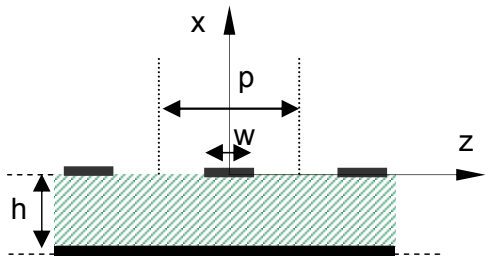

$$\left[Z_{yy}\left(k_{z0}^{TE}, f\right)\right](\mathrm{A}) = (0)$$

$$\left[Z_{zz}\left(k_{z0}^{TM}, f\right)\right](\mathrm{B}) = (0)$$

The Eigenvalues of the homogeneous linear system provide the **Propagation Constants** k^{TE}_{zn} (k^{TM}_{zn}), with n=0,±1, ± 2,…, of the spatial harmonics of TE_z (TM_z) modes as function of frequency

$$\mathrm{Det}\left[Z_{yy}\left(k_{z0}^{TE}, f\right)\right] = 0$$

$$\mathrm{Det}\left[Z_{zz}\left(k_{z0}^{TM}, f\right)\right] = 0$$

The propagation constant of each spatial harmonic is easily determined from the ***fundamental*** propagation constant

$$k_{zn} = k_{z0} + n2\pi/p = \beta_0 + n2\pi/p - j\alpha, \quad n = 0, \pm 1, \pm 2, \ldots$$

MSG-GDS as a Perturbation of Open and Closed Structures

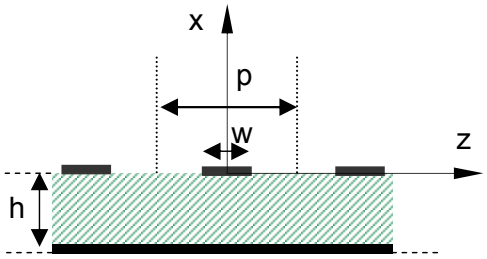

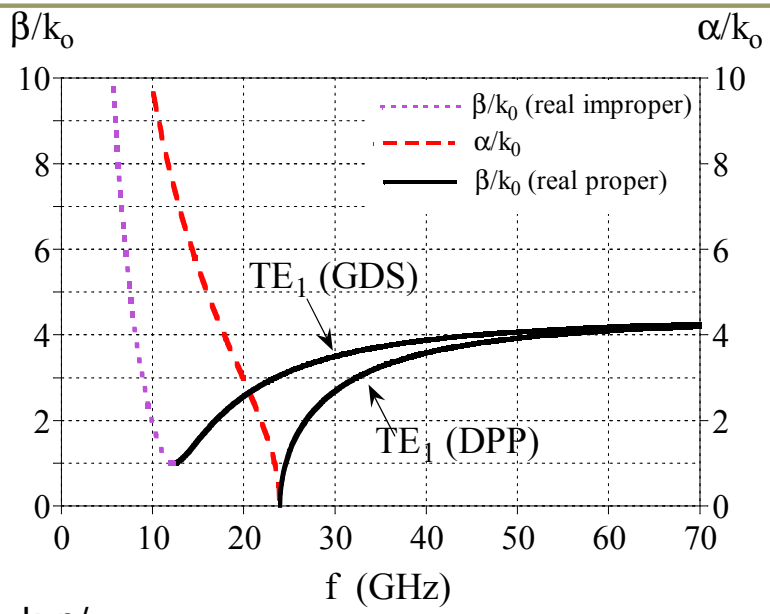

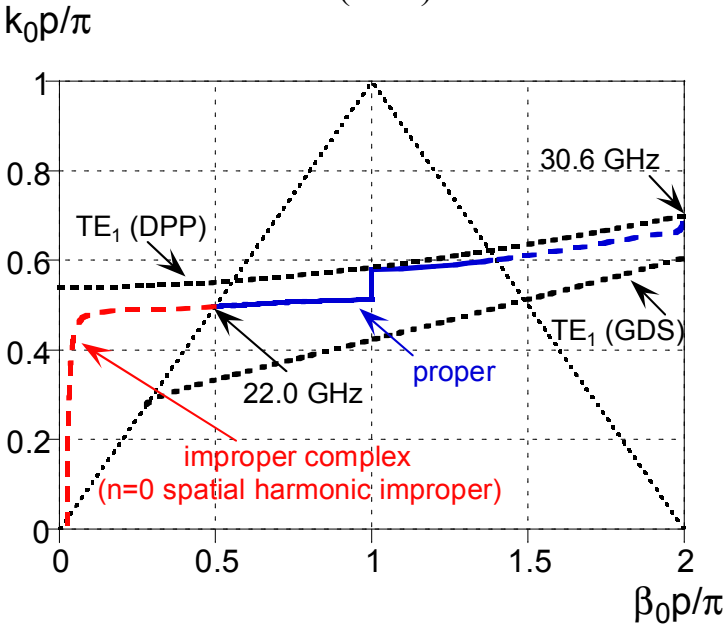

Grounded Dielectric Slab (GDS)

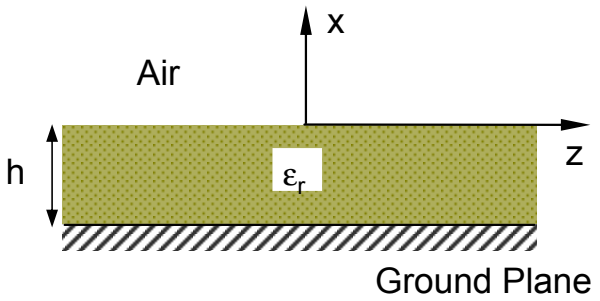

Dielectric-filled Parallel-Plate Waveguide (DPP)

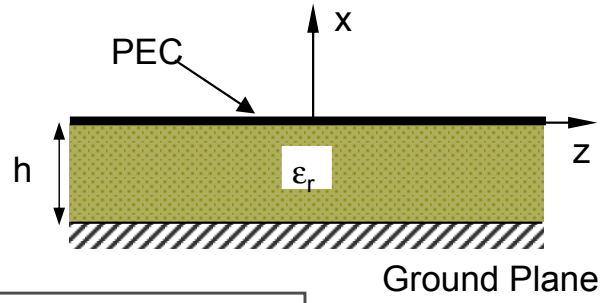

$\varepsilon_r = 20$, $h = 1.4$ mm,
$p = 3.38$ mm, $w/p = 0.6$

Mode Coupling in MSG-GDS: Pass Bands and Closed-Stop Bands

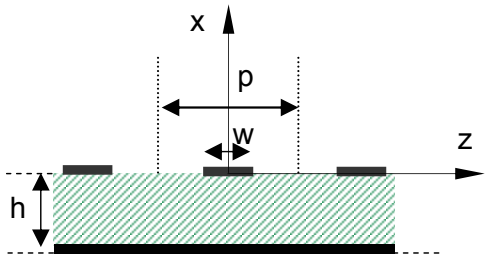

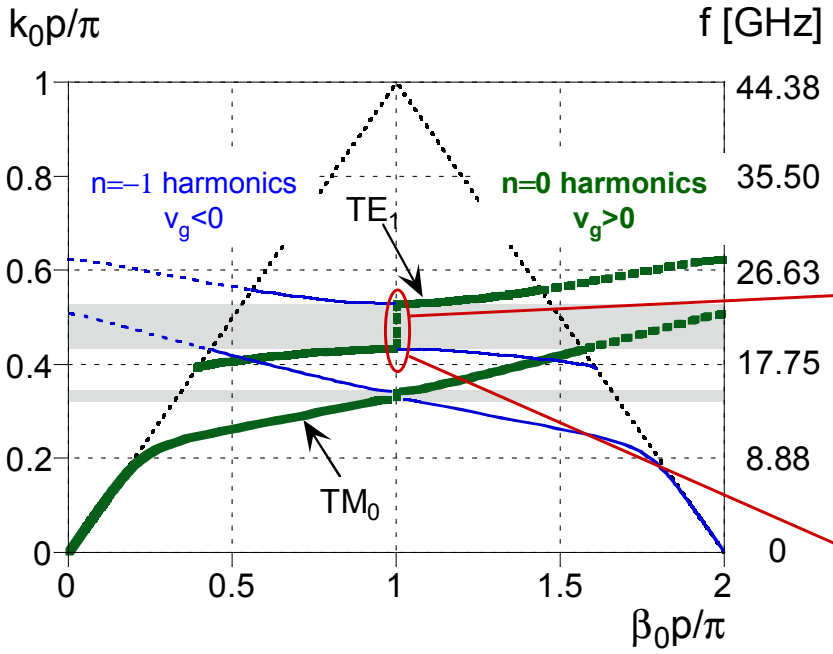

$$\beta_0 p = (2n+1)\pi$$
$$n = 0$$

Mode Coupling

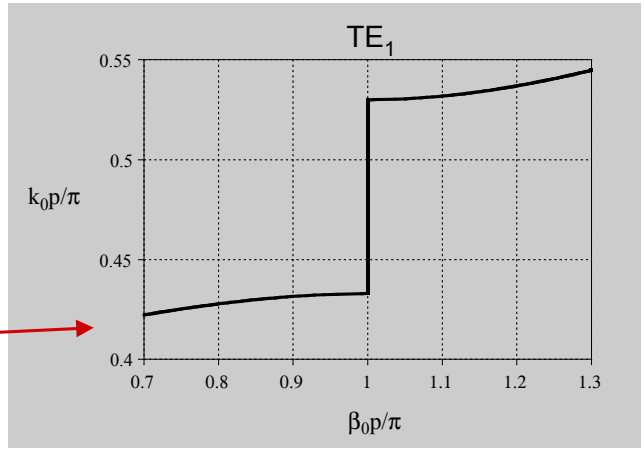

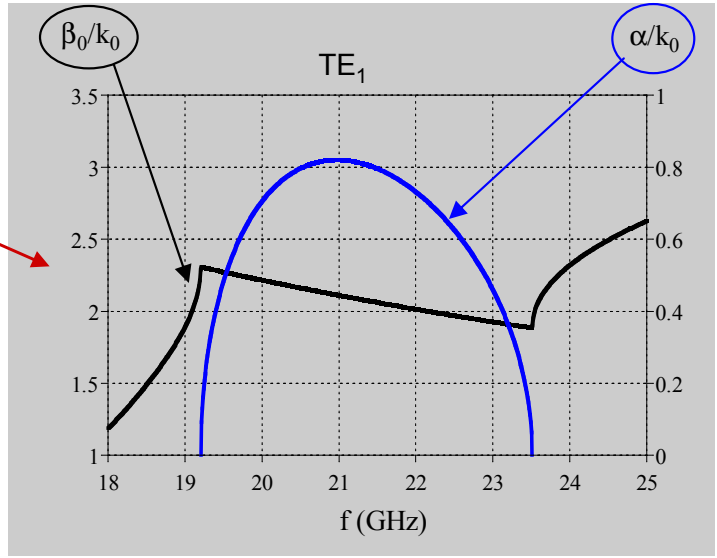

$$\varepsilon_r = 20 \ , \ h = 1.4 \text{ mm},$$
$$p = 3.38 \text{ mm}, \ w/p = 0.2$$

Highly Attenuated Bound Wave

MSG-GDS: Improper Transition Region

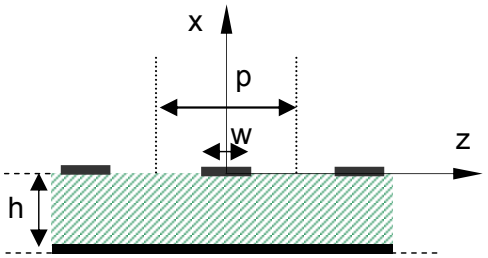

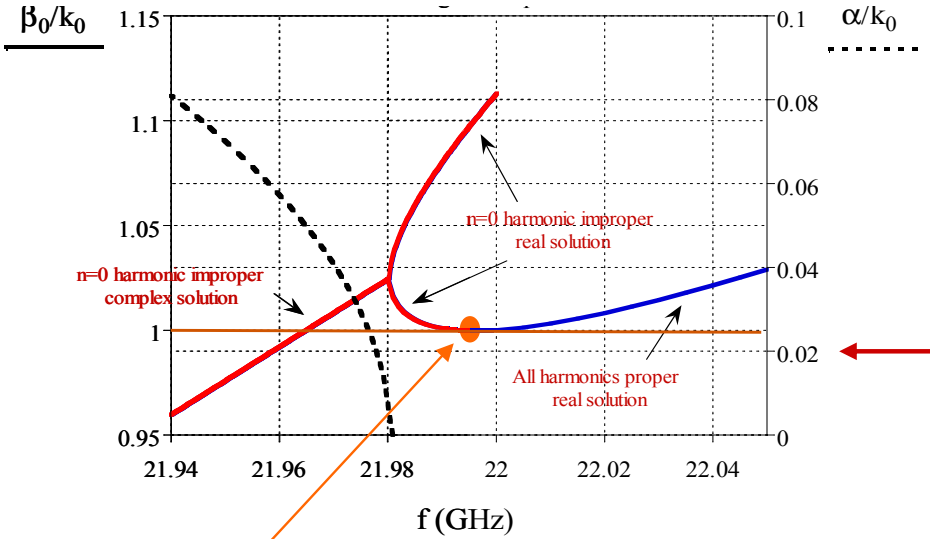

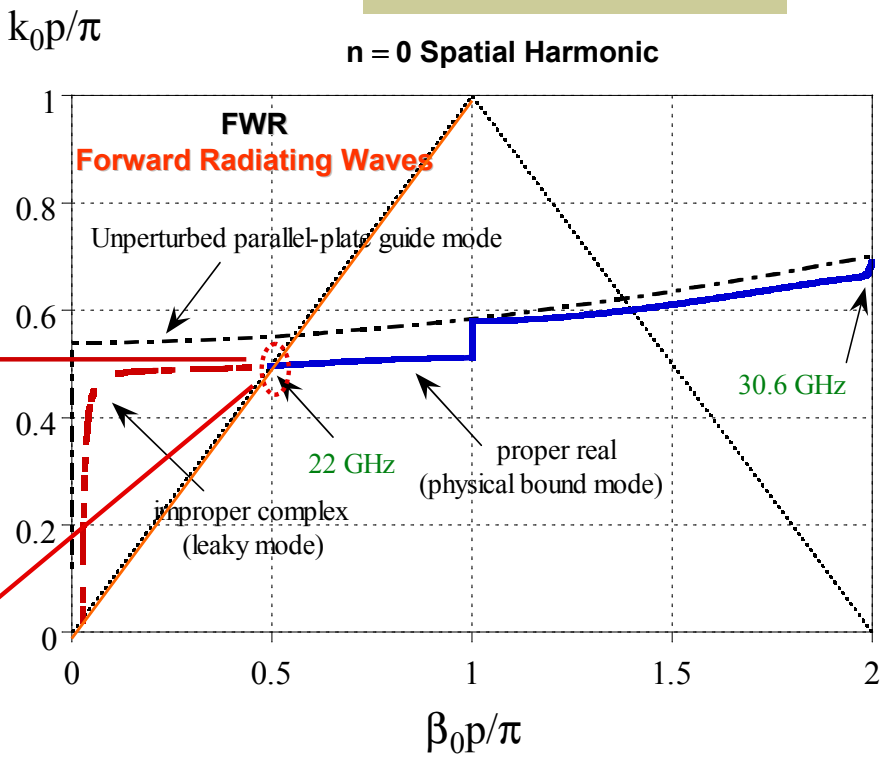

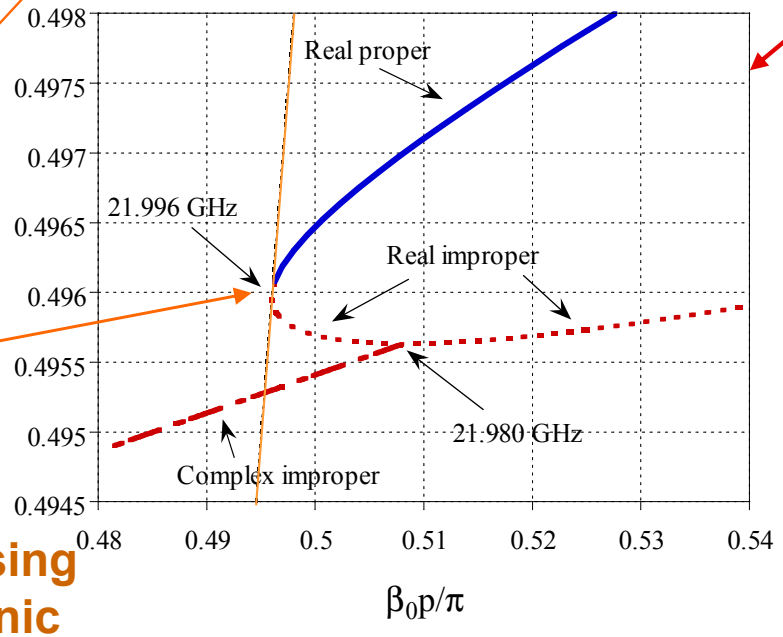

$$\begin{cases} \beta_0 = +k_0 \\ \alpha = 0 \end{cases}$$

Improper Spectral Gap

$$\varepsilon_r = 20 \ , \ h = 1.4 \text{ mm}, \quad p = 3.38 \text{ mm}, \ w/p = 0.6$$

Branch Point crossing for the n=0 harmonic

MSG-GDS: Proper Transition Region

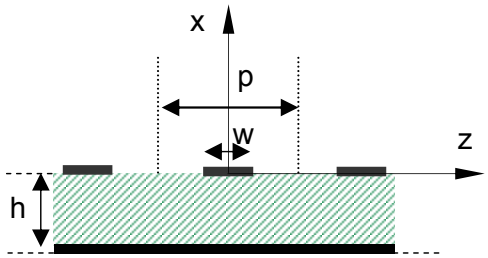

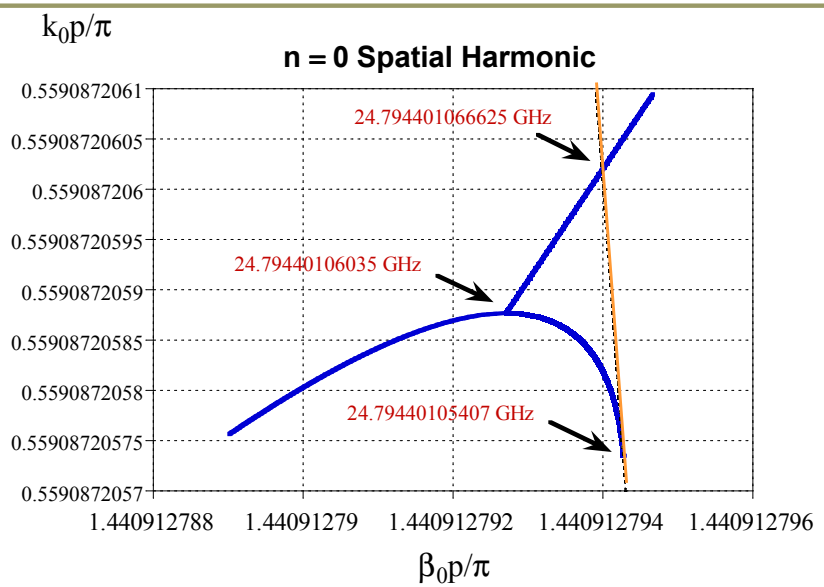

Proper Spectral Gap

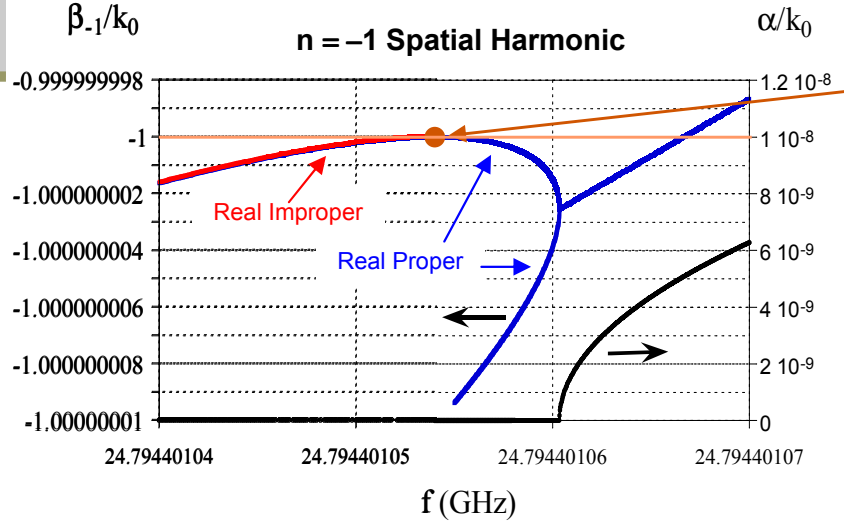

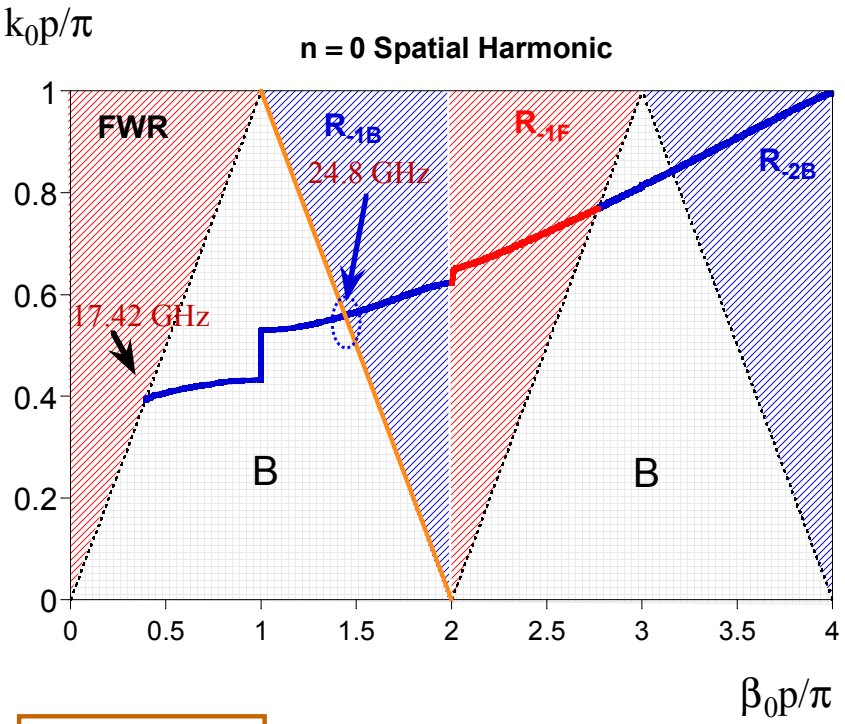

$$\begin{cases} \beta_{-1} = -k_0 \\ \alpha = 0 \end{cases}$$

Branch Point crossing for the n = - 1 harmonic

$$\varepsilon_r = 20 \ , \ h = 1.4 \text{ mm},$$
$$p = 3.38 \text{ mm}, \ w/p = 0.2$$

Mode Coupling in MSG-GDS: Open-Stop Band

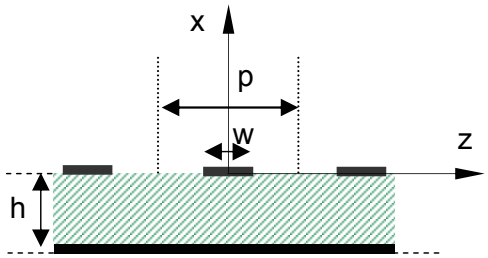

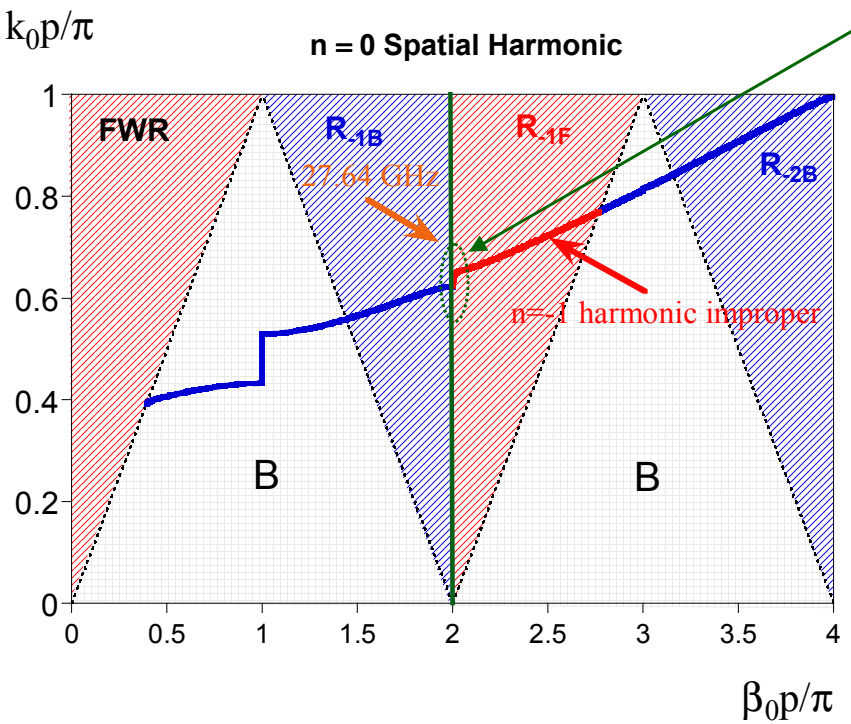

$$\beta_0 = \frac{2\pi}{p}$$

$$\beta_{-1} = 0$$

Branch Cut Crossing for the n = -1 harmonic

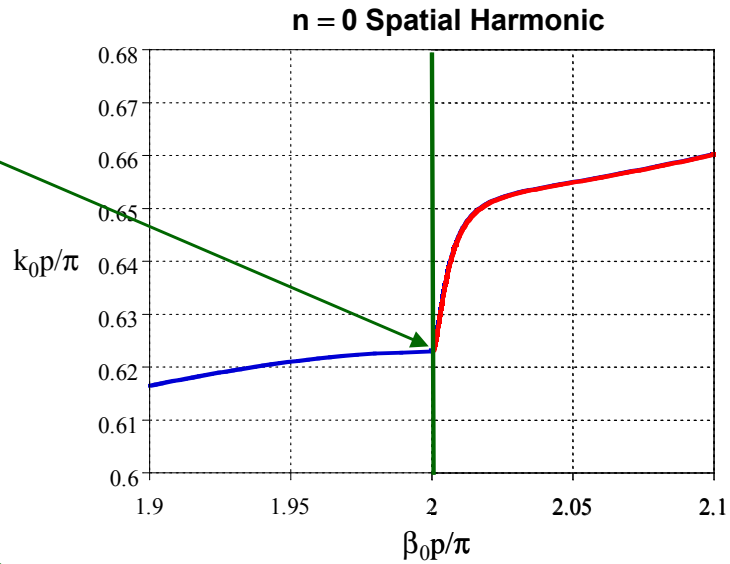

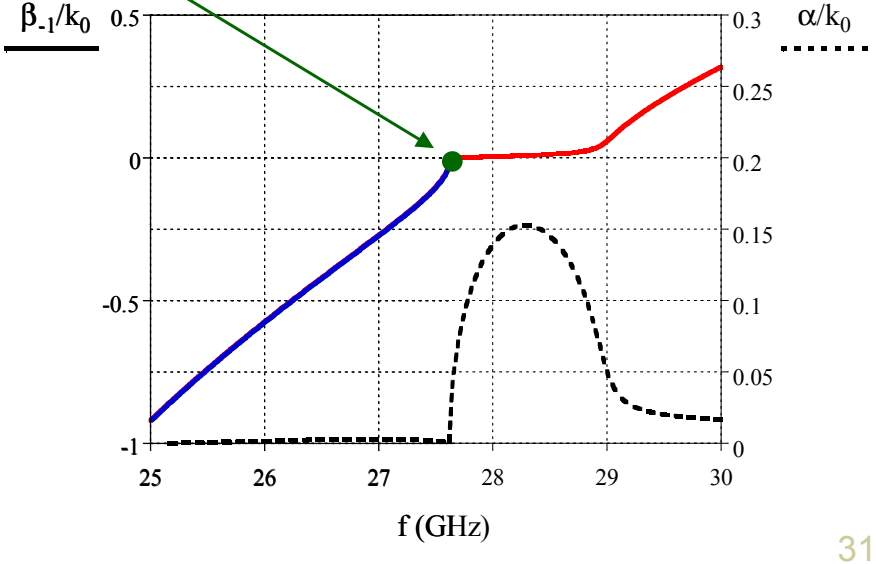

Open Stop Band: High Degradation of Radiation at Broadside

$\varepsilon_r = 20$, $h = 1.4$ mm,
p=3.38 mm, $w/p = 0.2$

Design of a printed leaky-wave 'bull-eye' antenna with suppressed surface-wave

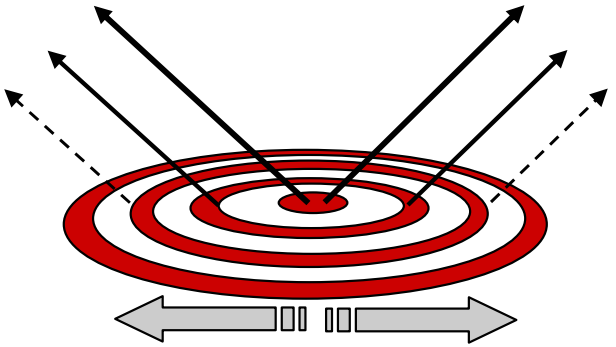

Paolo Baccarelli

"La Sapienza" University of Rome

Electronic Engineering Department

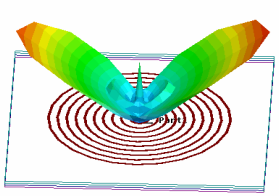

- A leaky-wave antenna based on a multiple-ring structure (bull-eye)
- This antenna is characterized by a high efficiency and reduced edge diffraction and operates on the n=-1 harmonic of the TM_0 mode
- A design procedure based on the dispersion behavior of an infinite 1D periodic linear array is presented
- Numerical results obtained through a commercial software (Ensemble^{TM}) on the radiated field are presented

Design technique (1)

We consider TM and TE modes with respect of the normal *z* direction

Infinite 'bull-eye' structure

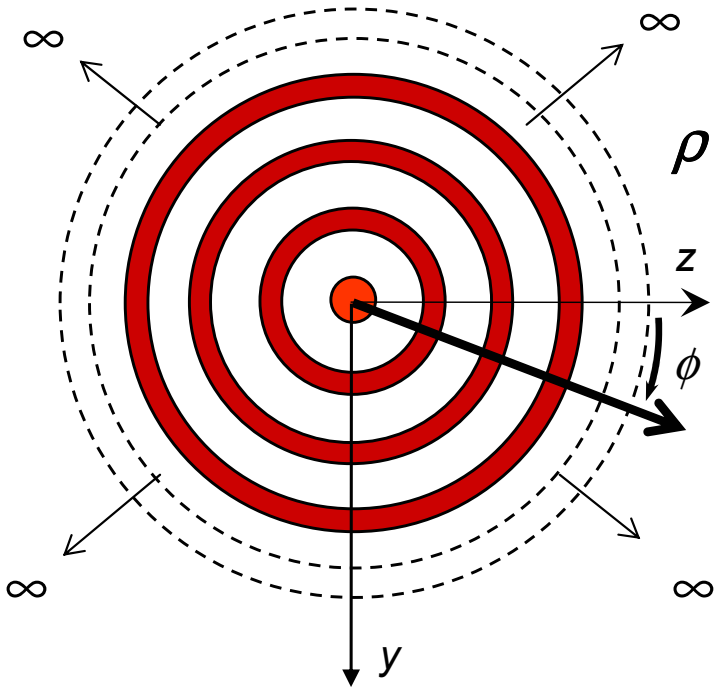

along ρ

≡

Infinite 1D periodic linear array of microstrips

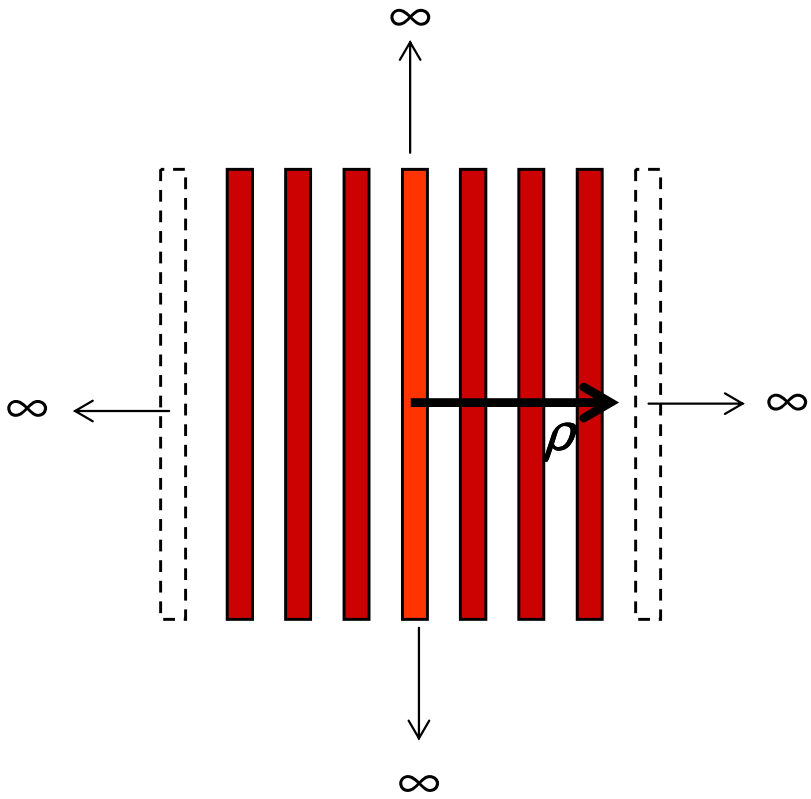

Beyond the near field: each mode has the same radial propagation constant $\boldsymbol{k}_\rho$ as the corresponding mode of linear array

‘Bull-eye’ antenna

- A series of concentric annular microstrip rings of width *w* and radial period *p*

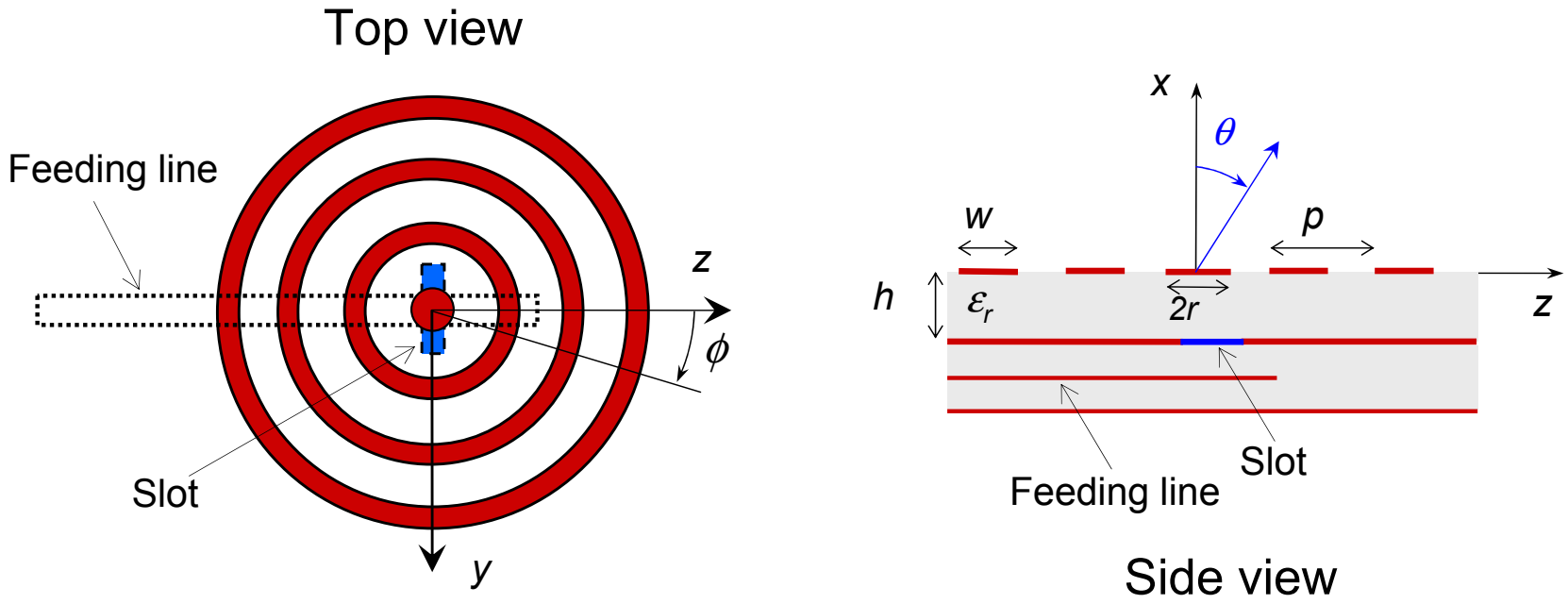

- Excitation through a rectangular slot etched on the ground plane

Design technique (1)

Aim: obtain a leaky-wave radiator in absence of any other physical leaky or surface wave

- The operation is based on the excitation of the fundamental TM_0 mode of the periodic structure
- Three possible operating mode when the TM_0 mode radiates
  1. TE_1 mode in stopband region
  2. TE_1 mode nonphysical
  3. Suppressed TE_1 surface-wave

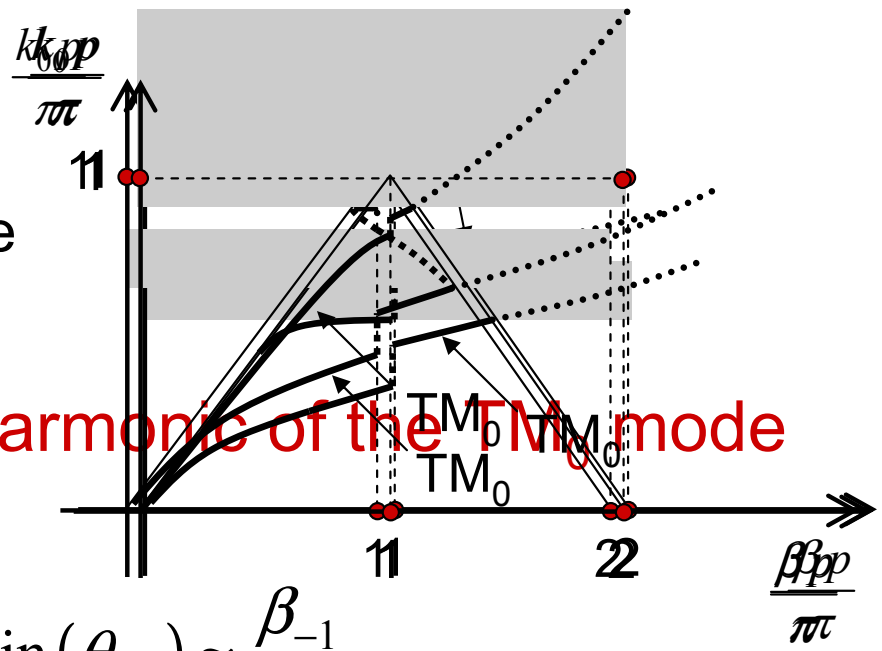

- Radiation through the n=-1 harmonic of the TM_0 mode in the backward quadrant:

$$-1 < \frac{\beta_{-1}}{k_0} < 0, \qquad \sin(\theta_M) \simeq \frac{\beta_{-1}}{k_0}$$

Design technique (2)

Operating mode 1

Shaded area [19.21-23.5] GHz

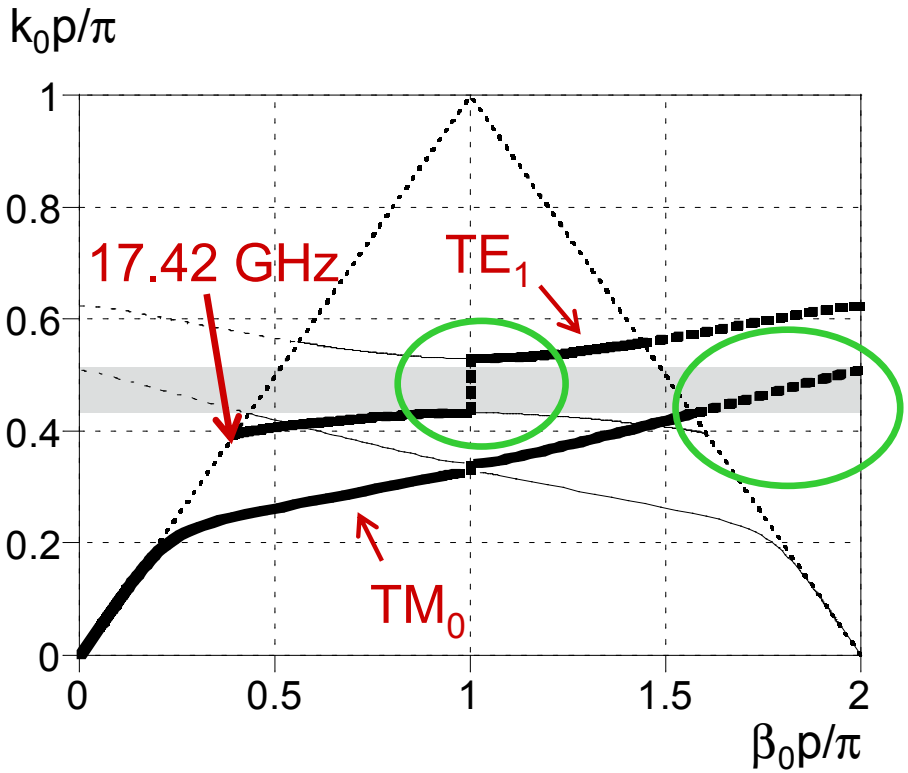

Structure parameters:

$\varepsilon_r = 20$	w/p = 0.2
d = 3.38 mm	h = 1.4 mm

Part of the radiative region of the TM_0 is superimposed to the TE_1 stopband region

Drawbacks

1. Very high dielectric constant (not suitable for antenna substrates)
2. The TE_1 stopband region could be very narrow

Design technique (3)

Operating mode 2

Shaded area [20.55-25.14] GHz

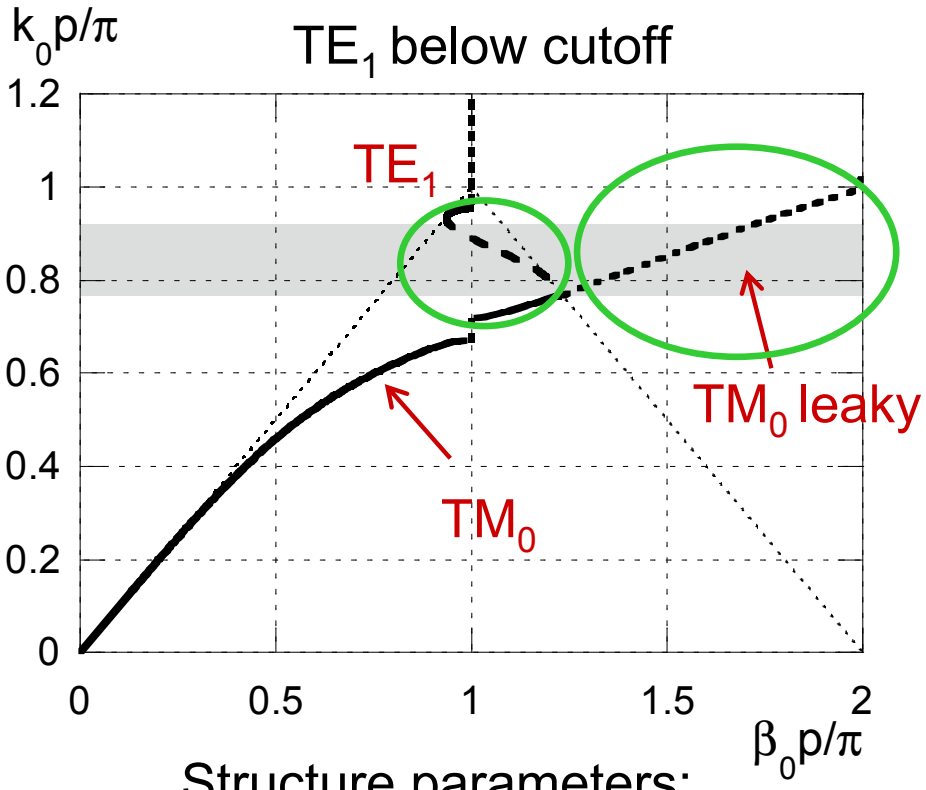

Structure parameters:

$\varepsilon_r = 6.8$ *w/p* = 0.2

d = 5.6 mm *h* = 1.4 mm

When the TM_0 mode radiates the TE_1 mode is in a non physical region (real improper solution)

Drawbacks

1. High dielectric constant (not suitable for antenna substrates)
2. The TM_0 radiative region and the TE_1 nonphysical region are superimposed only in a narrow frequency range.

Design technique (4)

- Substrates employed in leaky-wave planar antenna design typically are $2 < \varepsilon_r < 4$

- For substrates with low dielectric constant TM_0 starts to radiate closer to the top of the triangle

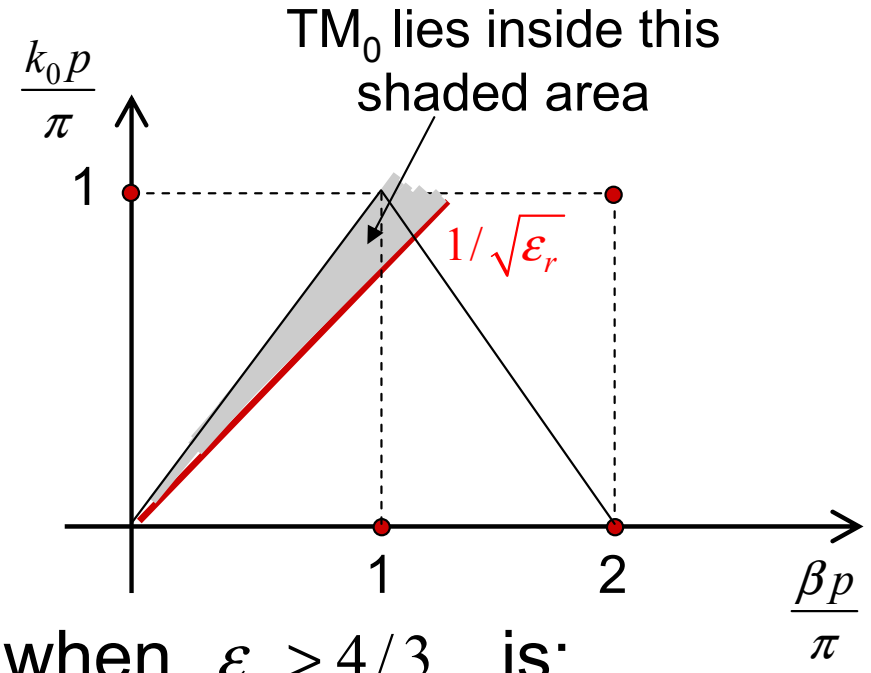

- The cutoff of the TE_1 mode when $\varepsilon_r > 4/3$ is:

Grounded slab — TE_1 cutoff — Parallel-plate waveguide

$$\frac{c}{4h\sqrt{\varepsilon_r - 1}} < f^{TE_1} < \frac{c}{2h\sqrt{\varepsilon_r}}$$

Design technique (5)

- In order to have surface-wave suppression for TE_1 we impose:

$$\frac{c}{4h\sqrt{\varepsilon_r - 1}} > f_0$$

where f_0 corresponds to the top of the triangle

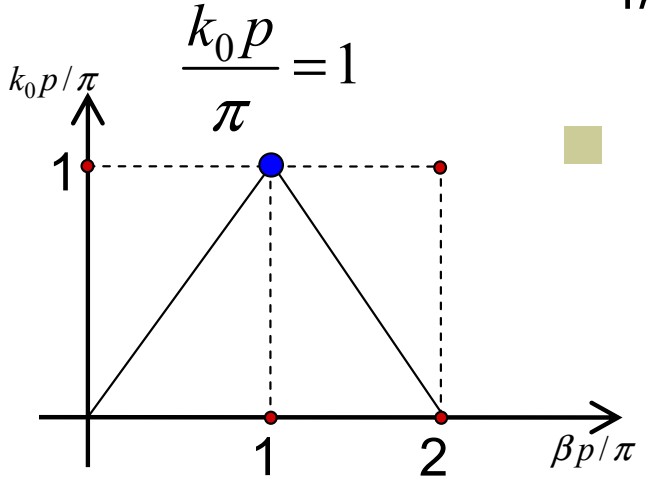

- From the relation between f_0 and the period p at the top of the triangle:

$$p = \frac{c}{2f_0} \Rightarrow \boxed{h < \frac{p}{2\sqrt{\varepsilon_r - 1}}}$$

- In order to avoid grating lobes: when $\beta_0 d / \pi = 2$

$$\frac{\beta_{-2}}{k_0} < -1 \Rightarrow \boxed{p < \lambda_0|_{BS}}$$

at broadside

Numerical results (1)

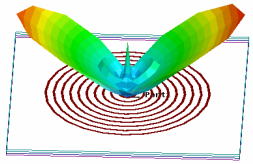

At ϕ=90° far field is mainly due to TE modes. No directive beams are present in this plane because TE modes are avoided.

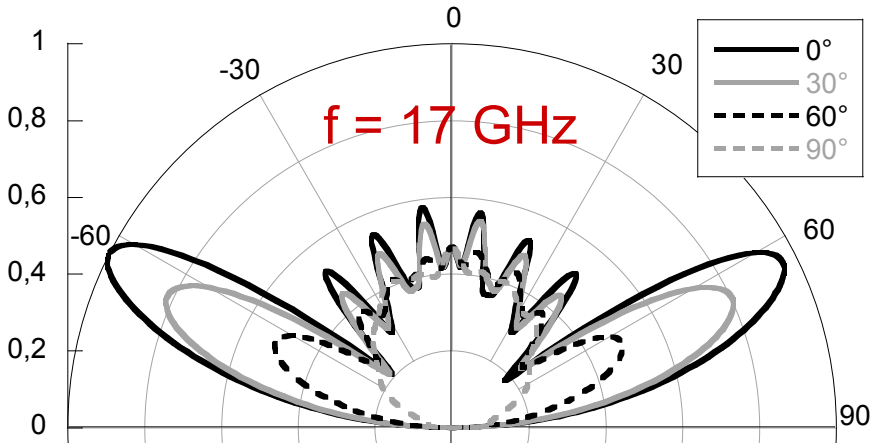

10 elements

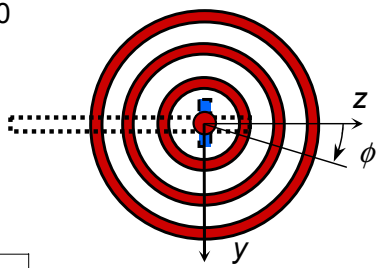

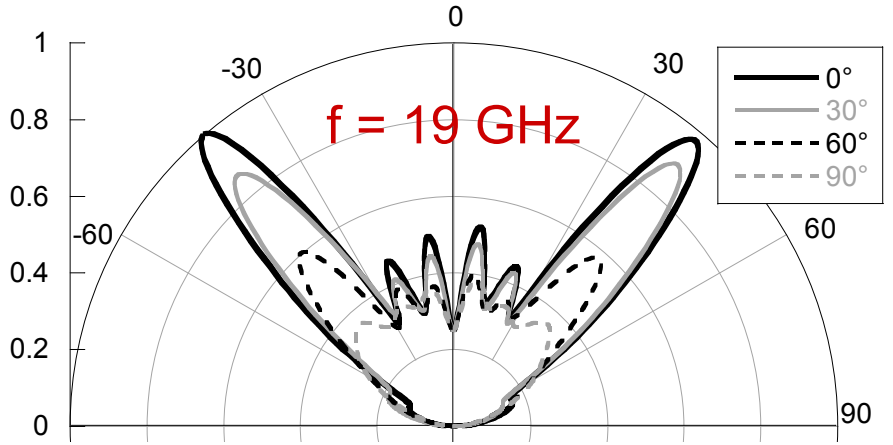

9 elements

Structure parameters:

$\varepsilon_r = 3.6$ w = 3.15 mm

p = 7 mm h = 2.7 mm

Numerical results (2)

Cutoff of TE_1 outside the triangle

TE_1 slab $\dfrac{c}{4h\sqrt{\varepsilon_r - 1}} \simeq 15.19$ GHz

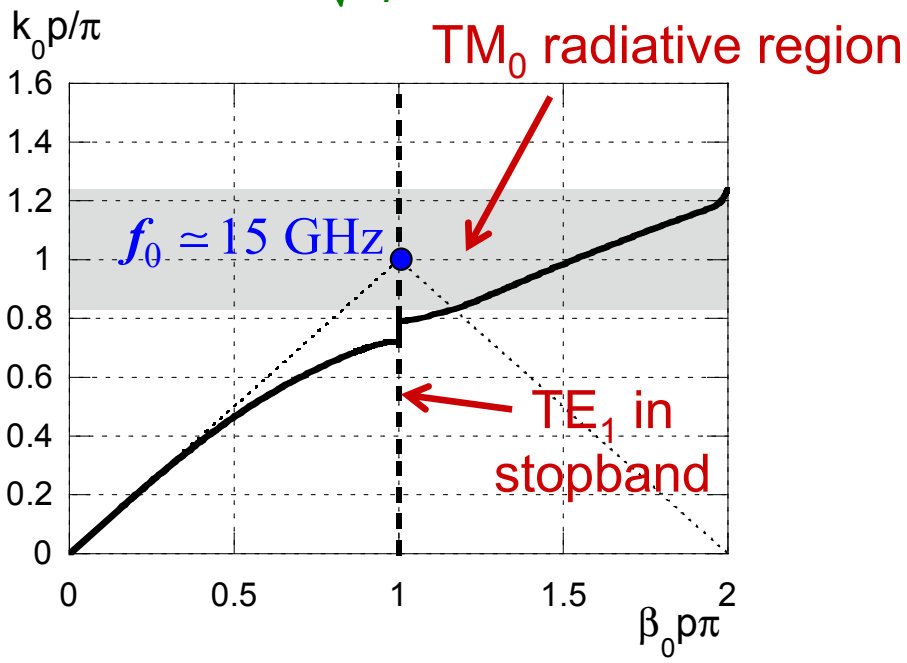

Structure parameters:

$\varepsilon_r = 4$	w = 3 mm
p = 10 mm	h = 2.85 mm

Dispersion diagram for the n=-1 harmonic

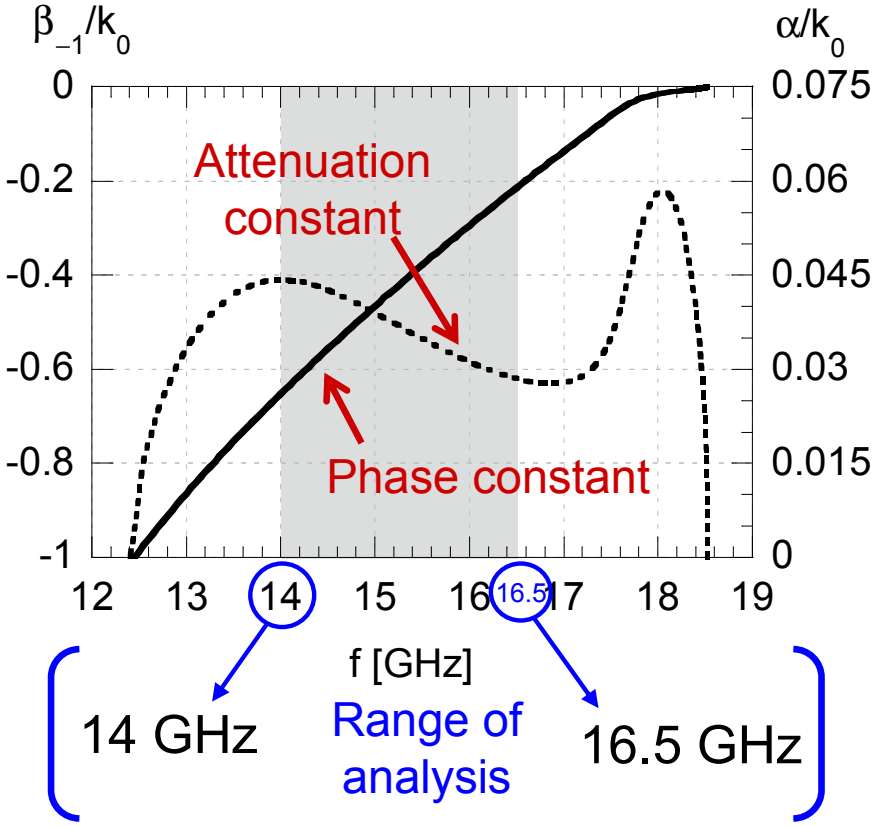

Inside this frequency range the attenuation constant is slow varying

Numerical results (3)

Wide angular scanning $\left[12.5° - 42° \right]$ $\theta_M^{LW} \simeq \theta_M^{ENS}$

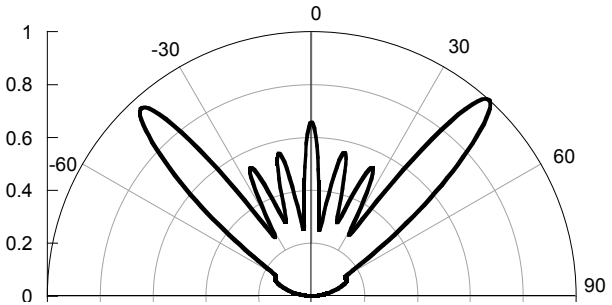

f=14 GHz

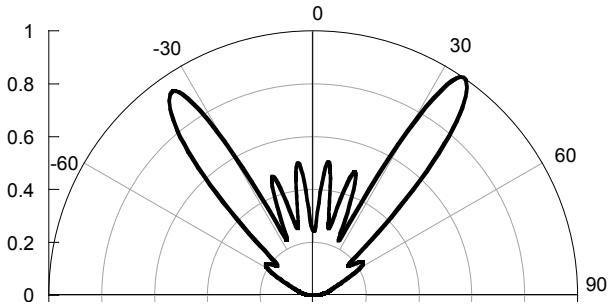

f=14.5 GHz

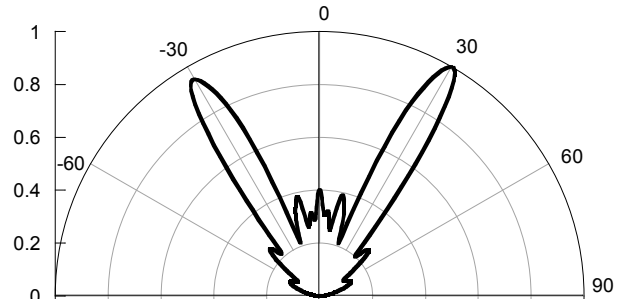

f=15 GHz

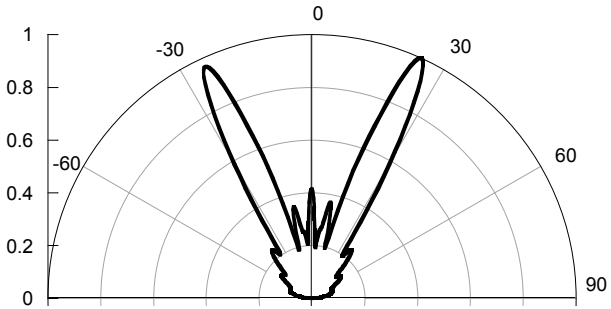

f=15.5 GHz

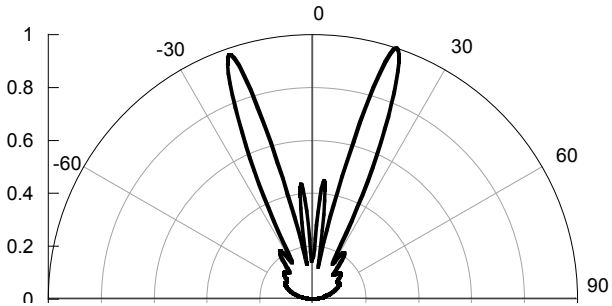

f=16 GHz

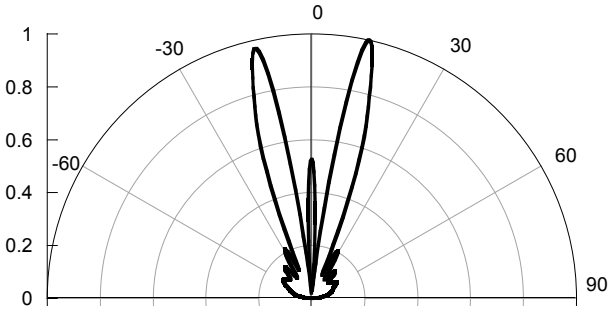

f=16.5 GHz

10 elements simulation

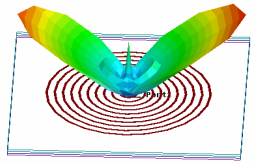

- A microstrip leaky-wave antenna has been designed, based on the excitation on a series of concentric, radially-periodic annular rings of the fundamental TM_0 mode in a leaky regime.
- By properly designing the physical and geometrical parameters of the structure, it is possible to avoid the presence of any other mode in a guided regime or in a physical leaky regime.
- High radiation efficiency and low edge-diffraction effects are expected and numerically verified from the performance of practical finite structures.

Axially Periodic 3D Structure: A Periodically Loaded Microstrip Line

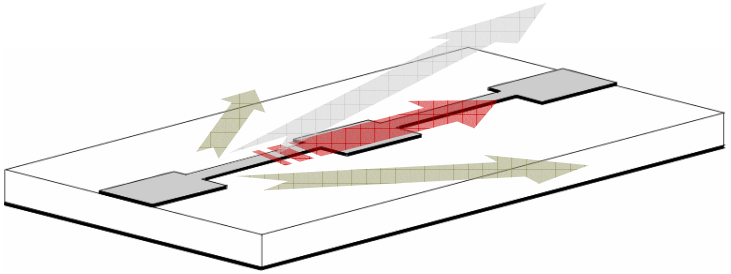

Paolo Baccarelli

"La Sapienza" University of Rome

Electronic Engineering Department

Axially Periodic Printed Lines

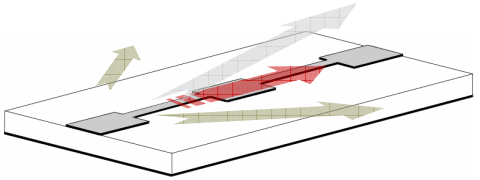

Unit Cell

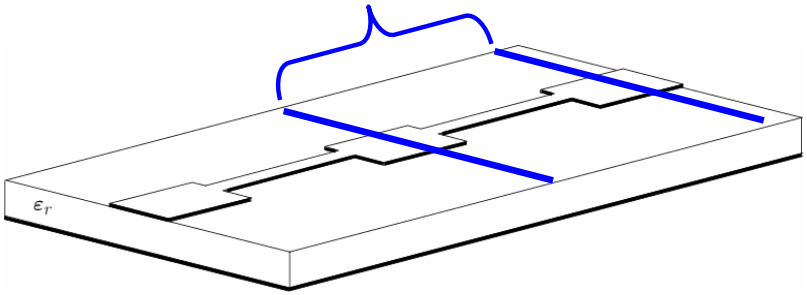

Unit Cell

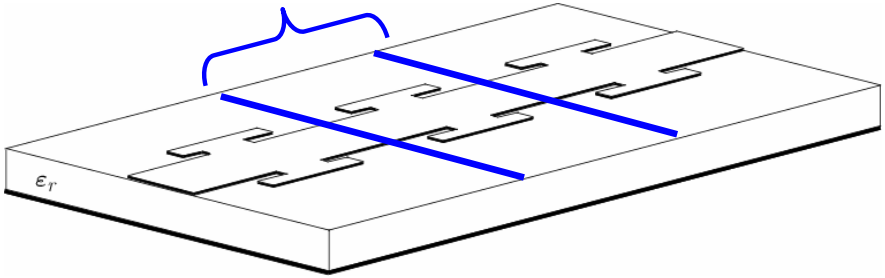

- Axially Periodic Printed Lines: Linear array of patches, periodically loaded microstrip lines (Filters, Leaky-Wave Antennas, 'Metamaterials')
- Modal Analysis (*infinite* array hypothesis): Unit-Cell Method and Spatial Harmonic Expansion (Floquet)
- ***Arbitrary*** Geometry of the metallization within the Unit Cell: Method of Moments in the Space Domain, Rao-Wilton-Glisson (RWG) triangular Basis Functions

Method of Moments in the Space Domain

Mixed Potential Integral Equations (MPIE)

MPIE

$$\underline{x}_o \times \left\{ -j\omega \int_S \left[G_A^p\left(\underline{r},\underline{r}'\right)\left(\underline{y}_o\underline{y}_o + \underline{z}_o\underline{z}_o\right)\right]\cdot \underline{J}^S\left(\underline{r}'\right)dS' - \nabla \int_S K_\Phi^p\left(\underline{r},\underline{r}'\right)\left[\nabla'\cdot \underline{J}^S\left(\underline{r}'\right)\right]dS' \right\} = \underline{0}$$

Discretization of **arbitrary geometry** within the ***unit cell***

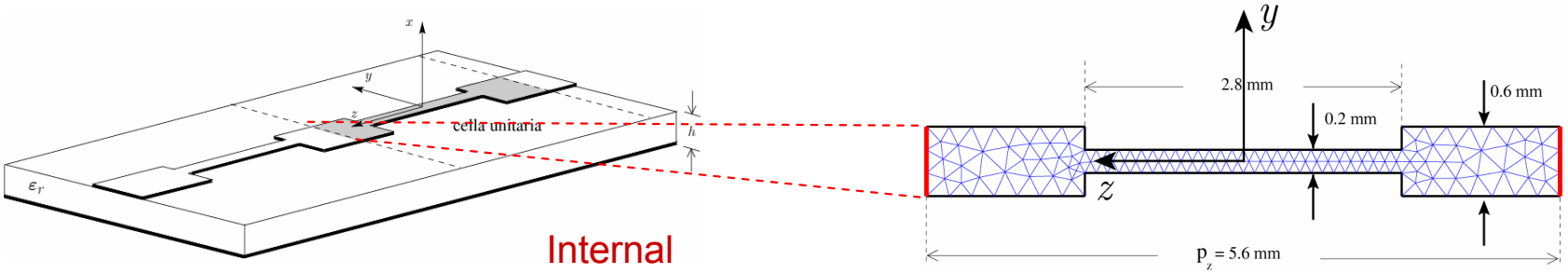

RWG

Internal Edges

$$\underline{J}_s \cong \sum_{n=1}^{N} I_n \underline{\Lambda}_n = \sum_{n=1}^{N_c} I_n^c \underline{\Lambda}_n + \sum_{n=1}^{N_{uc}} I_n^{uc} \underline{\Lambda}_n^{uc}$$

Edges on one of the Unit-Cell Borders

Reaction Integrals

$$\int_S \underline{\Lambda}_m\left(\underline{r}\right)\cdot \int_S \underline{\Lambda}_n\left(\underline{r}'\right) G_A^p(\underline{r},\underline{r}')\, dS'dS$$

$$\int_S \underline{\Lambda}_m\left(\underline{r}\right)\cdot \nabla \int_S \nabla'\cdot \underline{\Lambda}_n\left(\underline{r}'\right) K_\Phi^p(\underline{r},\underline{r}')\, dS'dS$$

Continuity through the Unit-Cell Borders

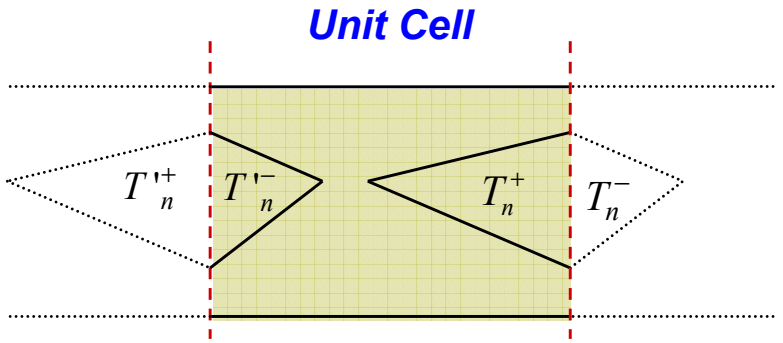

Correspondence between the Unit-Cell border Edges

Mixed Potentials (1)

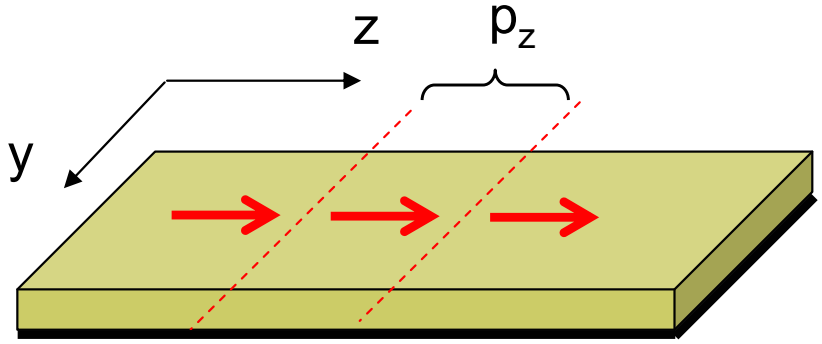

Periodicity along the axial direction *z*

$$J^p_{y,z}(y,z)=\delta(y)\frac{1}{p}\sum_{n=-\infty}^{+\infty} e^{-jk_{zn}z}$$

Floquet

$$k_{zn}=k_{z0}+\frac{2\pi n}{p}=\beta_0+\frac{2\pi n}{p}-j\alpha=\beta_n-j\alpha$$

$$\beta_n=\beta_0+\frac{2\pi n}{p},\quad n=0,\pm1,\pm2,..$$

1D Periodic Green Function

$$G^p_A(y,z)=G_A(y,z)\otimes J^p_{y,z}(y,z)$$

$$\tilde{G}_A(k_y,k_z)=\frac{1}{j\omega}V^{TE}(k_y,k_z)$$

$$\tilde{J}^p_{y,z}(k_y,k_z)=\frac{1}{p_z}\sum_{n=-\infty}^{+\infty}\delta(k_z-k_{zn})$$

$$G^p_A(y-y',z-z')=\frac{1}{(2\pi p)}\sum_{n=-\infty}^{+\infty} e^{-jk_{zn}(z-z')}\int_{-\infty}^{+\infty}\tilde{G}_A(k_y,k_{zn})e^{-jk_y(y-y')}dk_y$$

Series of an infinite number of Spectral Integrals

Singularity in $y-y'=z-z'=0$

The Modified Brillouin Diagram

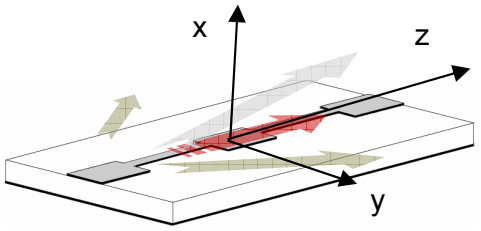

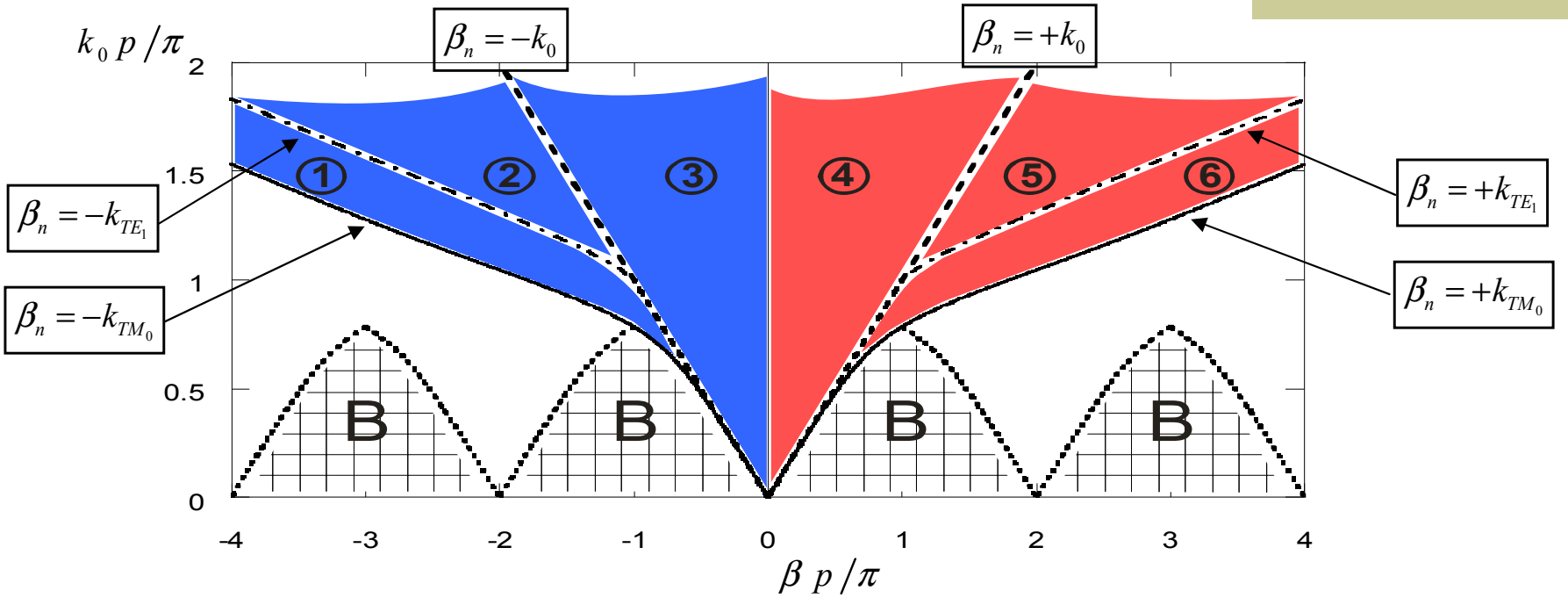

- An open 1-D periodic microstrip line is characterized by unbounded cross-sections along *x* and *y* directions: ***Space*** and ***Surface*** Leaky-Wave Regimes of both the ***Proper*** and ***Improper*** kinds exist
- ***New Radiation Regions*** (1,2,5,6) are depicted in the Brillouin diagram: Space Harmonics may radiate through the above cutoff ***surface waves*** of the ***background dielectric structure***

Guided Bloch-Wave

Integration Paths
in the Complex Plane

$$k_{zn} = \beta_n = \beta_0 + \frac{2\pi n}{p}, \quad n = 0, \pm 1, \pm 2, ..$$

$$|\beta_n| = \left|\beta_0 + \frac{2\pi n}{p}\right| < |k_{TM_0}|, \quad n = 0, \pm 1, \pm 2, ..$$

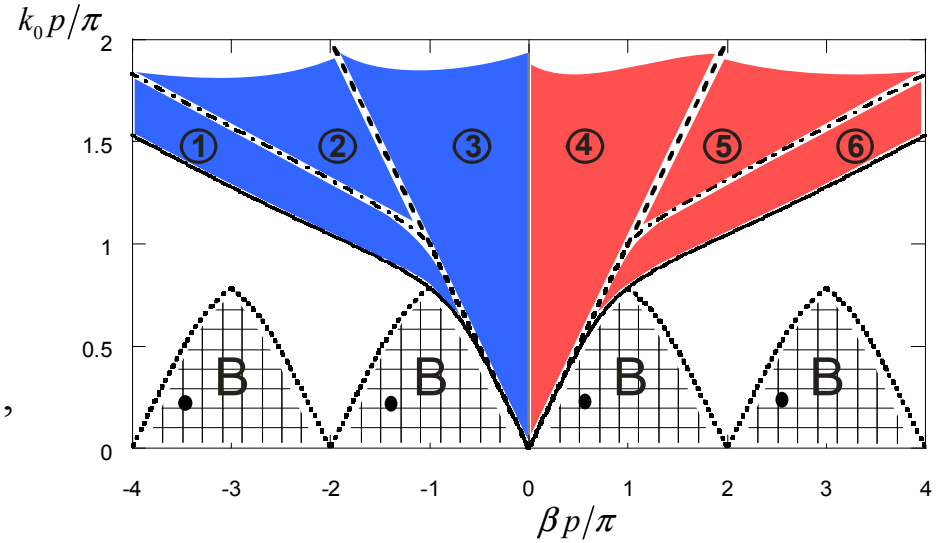

Each Spatial Harmonic Phase Constant is within Region **B**

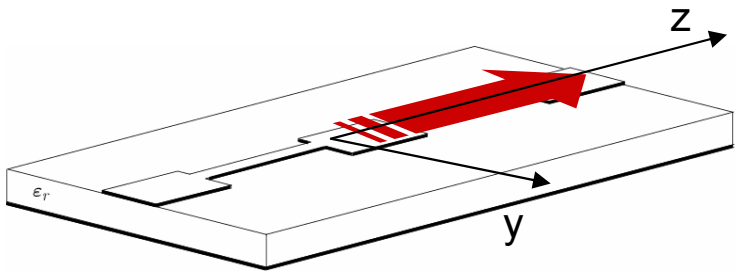

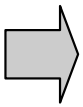

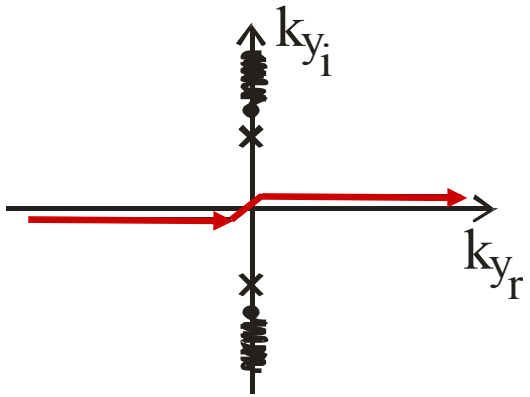

$$G_A^p\left(y-y', z-z'\right) = \frac{1}{(2\pi p)} \sum_{n=-\infty}^{+\infty} e^{-jk_{zn}\left(z-z'\right)} \int_{-\infty}^{+\infty} \tilde{G}_A\left(k_y, k_{zn}\right) e^{-jk_y\left(y-y'\right)} dk_y$$

The integration path is along the **real axis** on the proper sheet of the complex k_y plane for **all** the harmonics: **Proper Determination**

Closed-Stop Band Regime

Integration Paths in the Complex Plane

Each Spatial Harmonic Phase Constant is within Region **B**

$$|\beta_n| = \left|\frac{(2n+1)\pi}{p}\right| < |k_{TM_0}|,$$
$$n = 0, \pm 1, \pm 2, ..$$

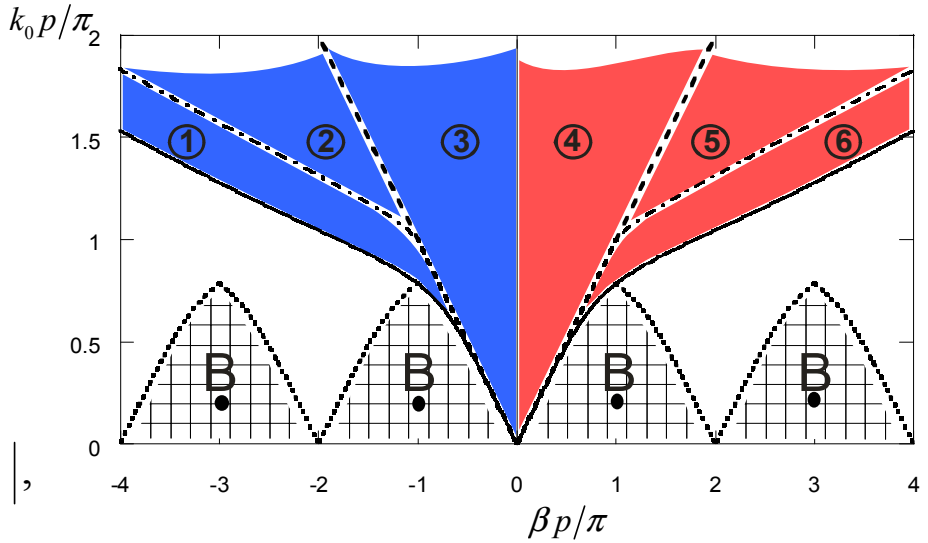

Complex Propagation Constant

$$k_{zn} = \beta_n - j\alpha,$$
$$n = 0, \pm 1, \pm 2, ..$$

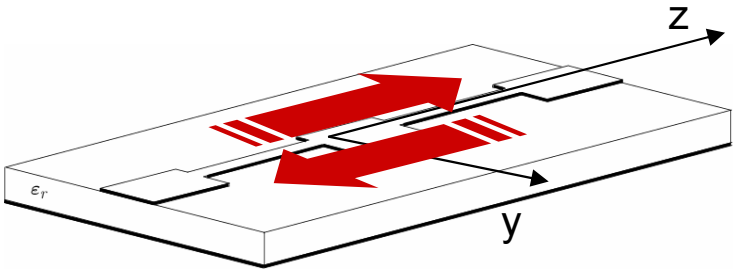

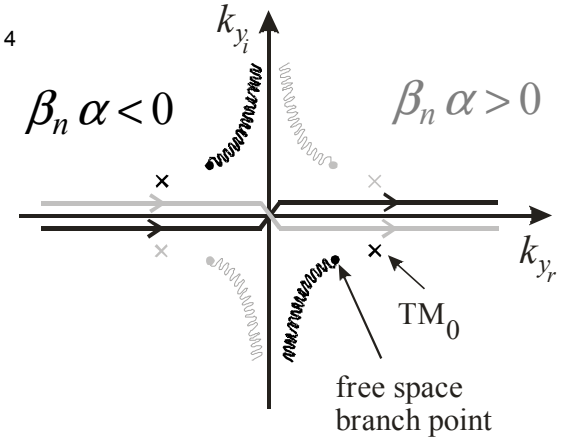

$$G_A^p(y-y', z-z') = \frac{1}{(2\pi p_z)} \sum_{n=-\infty}^{+\infty} e^{-jk_{zn}(z-z')} \int_{-\infty}^{+\infty} \tilde{G}_A(k_y, k_{zn})\, e^{-jk_y(y-y')}\, dk_y$$

The integration path is along the **real axis** on the proper sheet of the complex k_y plane for **all** the harmonics: **Proper Determination**

Backward Surface Leaky-Wave Regime

Integration Paths in the Complex Plane

At least One Spatial Harmonic Phase Constant is within Region:

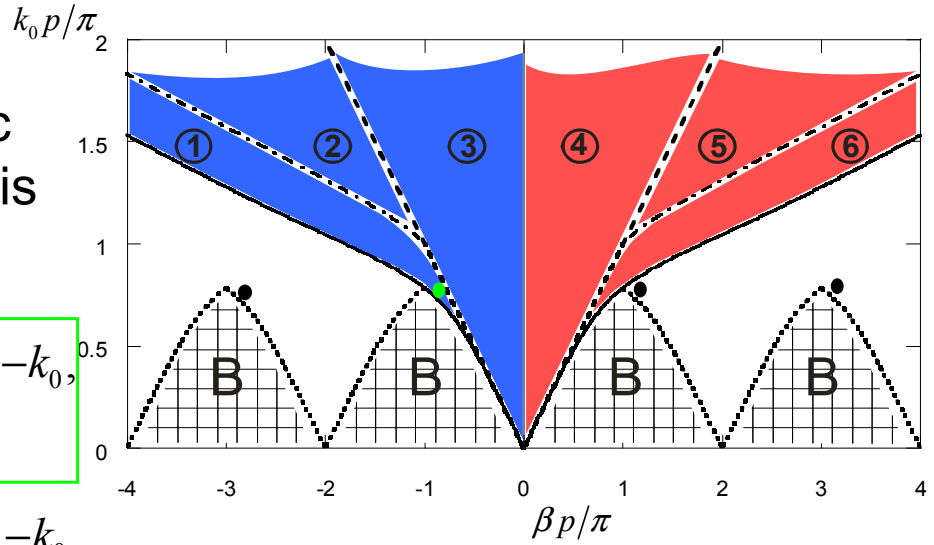

$$①:\begin{cases}-k_{TM_0}<\beta_n<-k_{TE_1}<-k_0,\\ n=0,\pm1,\pm2,..\end{cases}$$

$$②:\begin{cases}-k_{TM_0}<-k_{TE_1}<\beta_n<-k_0,\\ n=0,\pm1,\pm2,..\end{cases}$$

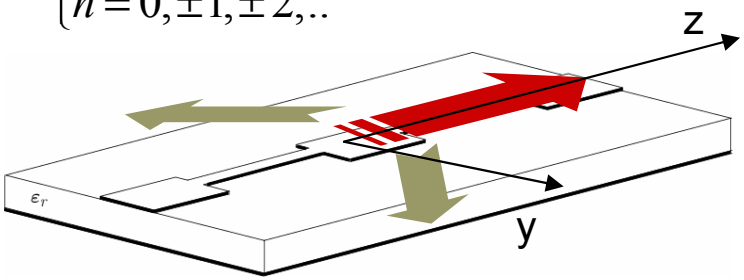

Complex Propagation Constant

$$k_{zn}=\beta_n-j\alpha,\quad n=0,\pm1,\pm2,..$$

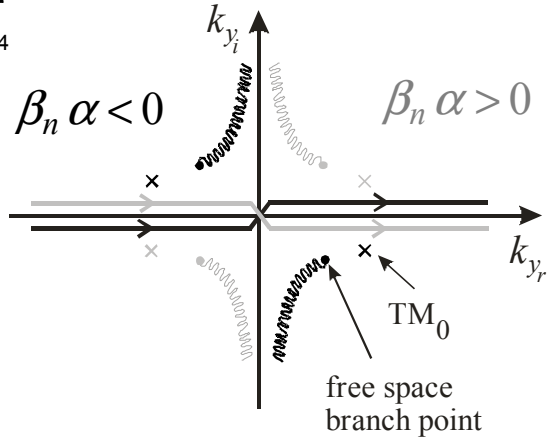

$$G_A^p\left(y-y',z-z'\right)=\frac{1}{\left(2\pi\,p_z\right)}\sum_{n=-\infty}^{+\infty}e^{-jk_{zn}\left(z-z'\right)}\int_{-\infty}^{+\infty}\tilde{G}_A\left(k_y,k_{zn}\right)e^{-jk_y\left(y-y'\right)}dk_y$$

The integration path is along the **real axis** on the proper sheet of the complex k_y plane for **all** the harmonics: **Proper Determination**

Backward Space Leaky-Wave Regime

Integration Paths in the Complex Plane

At least One Spatial Harmonic Phase Constant is within Region:

$$③ : \begin{cases} -k_0 < \beta_n < 0, \\ n = 0, \pm 1, \pm 2, .. \end{cases}$$

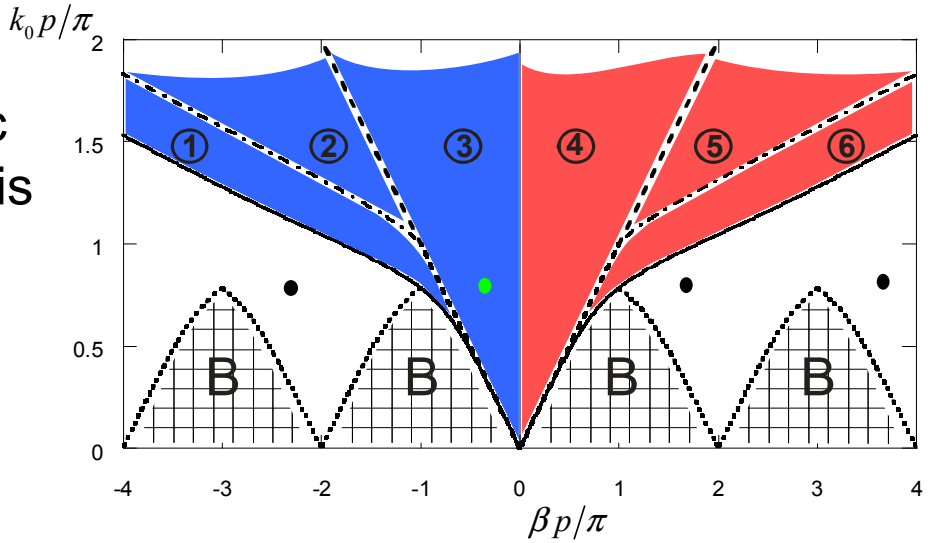

Complex Propagation Constant

$$k_{zn} = \beta_n - j\alpha,$$
$$n = 0, \pm 1, \pm 2, ..$$

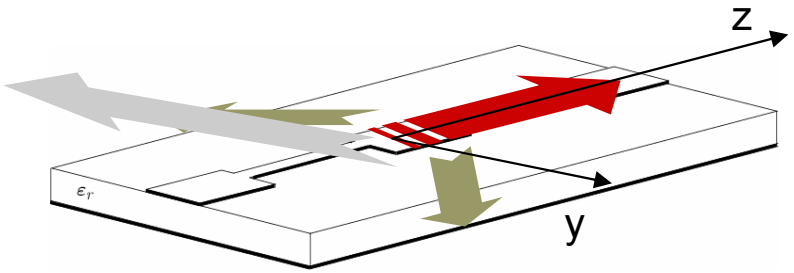

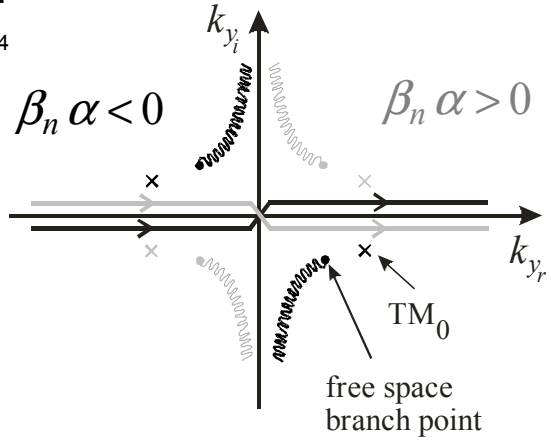

$$G_A^p\left(y-y', z-z'\right) = \frac{1}{(2\pi p_z)} \sum_{n=-\infty}^{+\infty} e^{-jk_{zn}\left(z-z'\right)} \int_{-\infty}^{+\infty} \tilde{G}_A\left(k_y, k_{zn}\right) e^{-jk_y\left(y-y'\right)} dk_y$$

The integration path is along the **real axis** on the proper sheet of the complex k_y plane for **all** the harmonics: **Proper Determination**

Forward Space Leaky-Wave Regime

Integration Paths in the Complex Plane

At least One Spatial Harmonic Phase Constant is within Region:

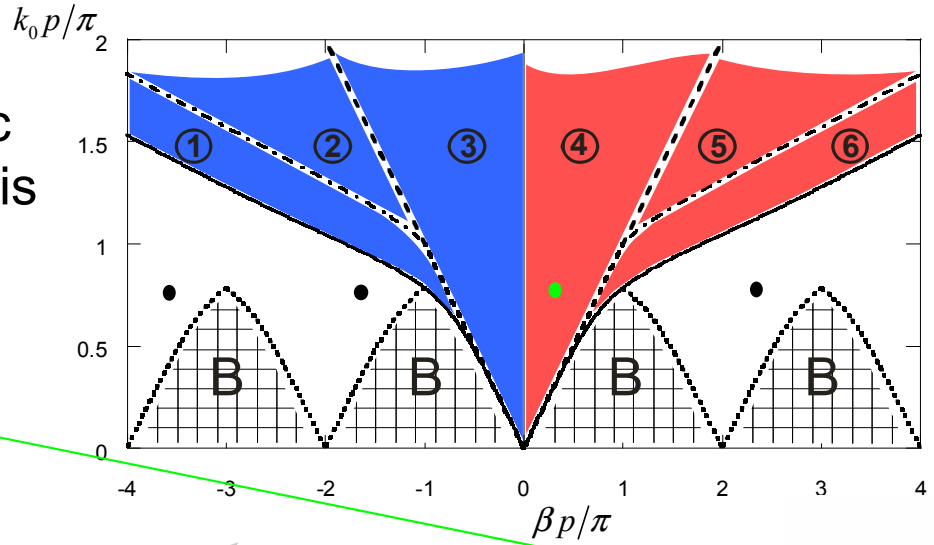

Complex Propagation Constant

$$k_{zn} = \beta_n - j\alpha,$$
$$n = 0, \pm 1, \pm 2, ..$$

$$④ : \begin{cases} 0 < \beta_n < k_0, \\ n = 0, \pm 1, \pm 2, .. \end{cases}$$

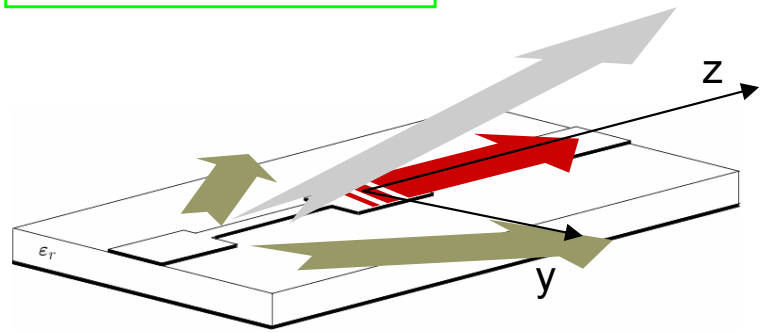

Improper Determination

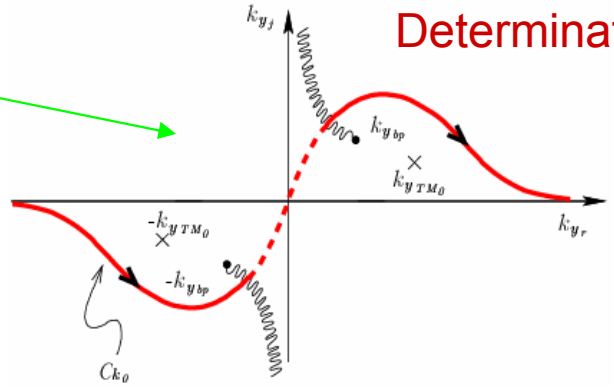

The integration path for any forward space radiating harmonic passes through the branch cuts and lies partially on the ***Bottom Sheet*** of the complex k_y plane

$$G_A^p\left(y-y',z-z'\right) = \frac{1}{\left(2\pi\, p_z\right)} \sum_{n=-\infty}^{+\infty} e^{-jk_{zn}\left(z-z'\right)} \int_{-\infty}^{+\infty} \tilde{G}_A\left(k_y,k_{zn}\right) e^{-jk_y\left(y-y'\right)} dk_y$$

Forward Surface Leaky-Wave Regime

Integration Paths in the Complex Plane

At least One Spatial Harmonic Phase Constant is within Region:

$$\text{⑤}: \begin{cases} k_0 < \beta_n < k_{TE_1} < k_{TM_0}, \\ n = 0, \pm 1, \pm 2, .. \end{cases}$$

$$\text{⑥}: \begin{cases} k_0 < k_{TE_1} < \beta_n < k_{TM_0}, \\ n = 0, \pm 1, \pm 2, .. \end{cases}$$

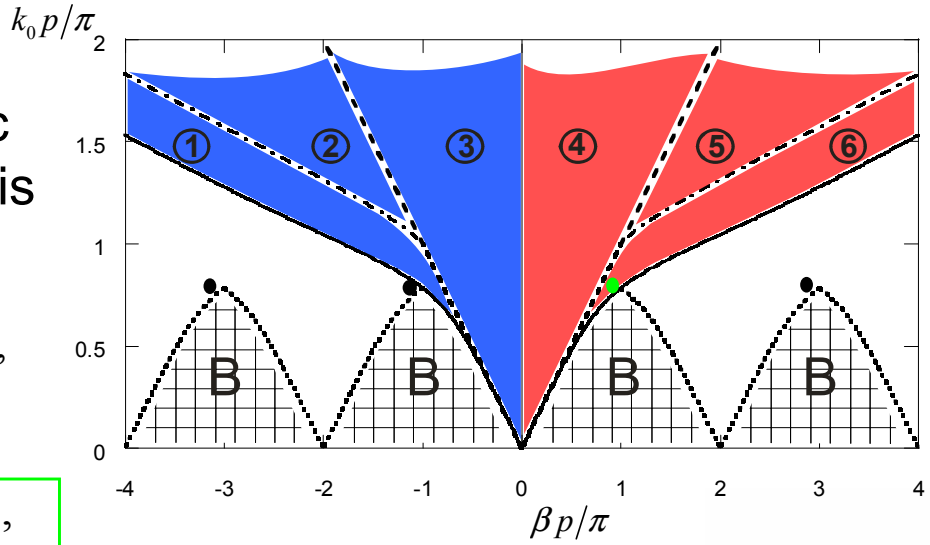

Complex Propagation Constant

$$k_{zn} = \beta_n - j\alpha,$$
$$n = 0, \pm 1, \pm 2, ..$$

Improper Determination

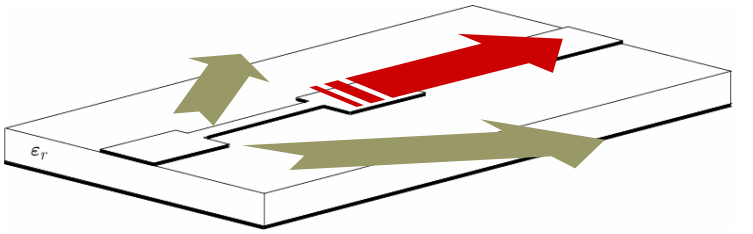

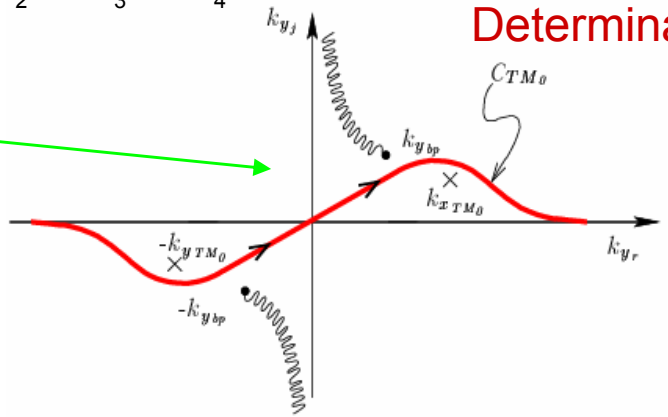

$$G_A^p\left(y-y', z-z'\right) = \frac{1}{\left(2\pi p_z\right)} \sum_{n=-\infty}^{+\infty} e^{-jk_{zn}\left(z-z'\right)} \int_{-\infty}^{+\infty} \tilde{G}_A\left(k_y, k_{zn}\right) e^{-jk_y\left(y-y'\right)} dk_y$$

The integration path for any forward surface leaky wave harmonic passes around the pole singularities on the complex k_y plane

Numerical results (4)

Parameters:

$\varepsilon_r = 10.2$ $\quad p = 4$ mm

$h = 0.676$ mm

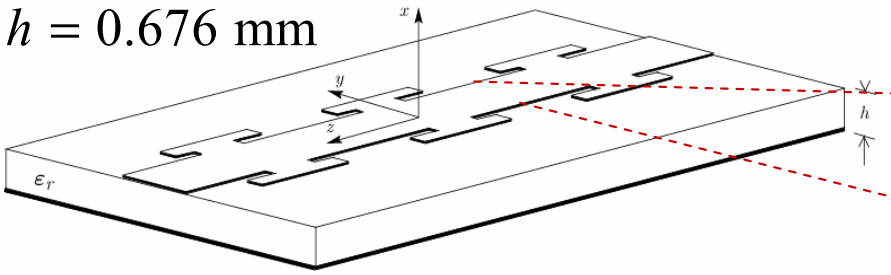

Unit Cell

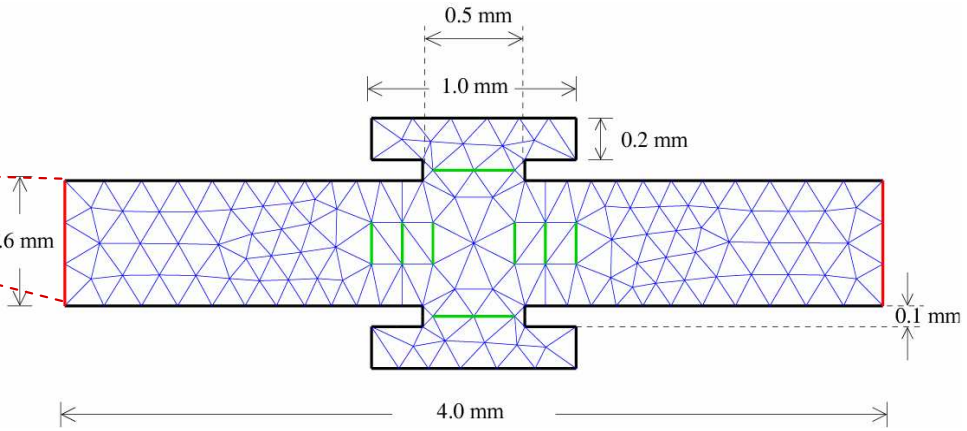

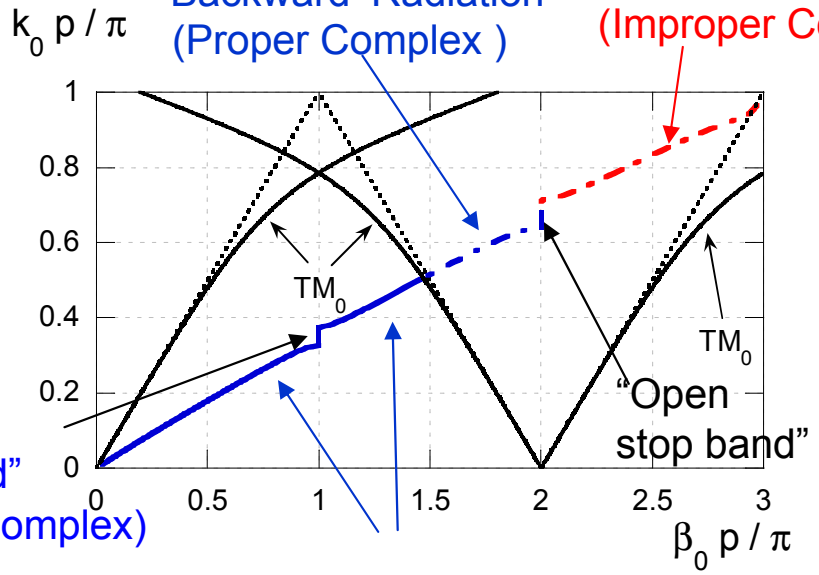

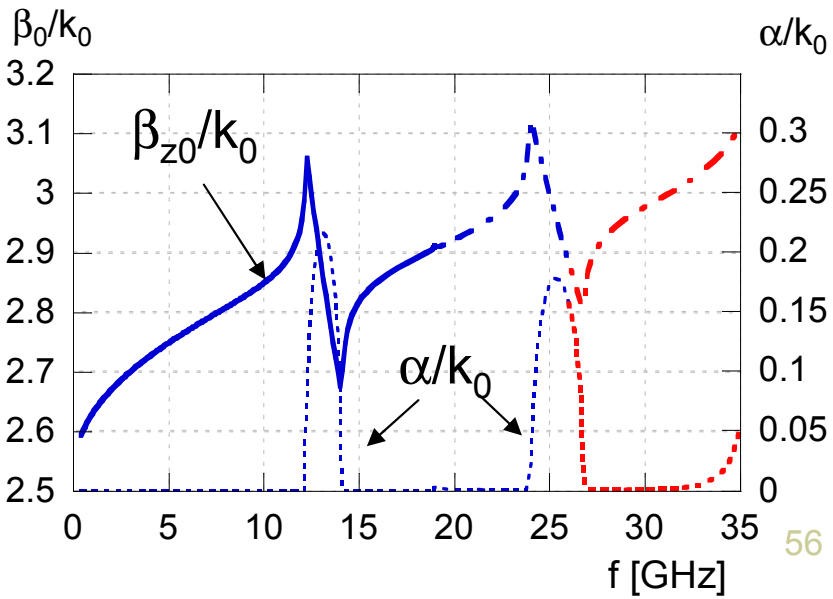

References

- R. E. Collin and F. J. Zucker (Eds.), *Antenna Theory*. New York, NY: McGraw- Hill, 1969, ch. 19
- R. E. Collin, *Field theory of guided waves*. Piscataway, NJ: IEEE Press, 2° ed., 1991, ch. 9
- A. F. Peterson, S. L. Ray e R. Mittra, *Computational methods for electromagnetics*. NJ: IEEE Press, 1997, ch. 7
- A. A. Oliner, "Radiating periodic structures: analysis in terms of k vs. β diagrams," *SHORT COURSE on Microwave Field and Network Techniques*, 4 June, 1963
- P. Burghignoli, P. Baccarelli, F. Frezza, A. Galli, P. Lampariello, and A. A. Oliner, "Low-frequency dispersion features of a new complex mode for a periodic strip grating on a grounded dielectric slab", *IEEE Transactions on Microwave Theory and Techniques*, vol. 49, pp. 2197-2205, Dec 2001
- P. Baccarelli, P. Burghignoli, C. Di Nallo, F. Frezza, A. Galli, P. Lampariello, and G. Ruggieri, "Full-wave analysis of printed leaky-wave phased arrays", International Journal of RF and Microwave Computer Aided Engineering, vol. 12, pp. 272-287, May 2002
- P. Baccarelli, P. Burghignoli, F. Frezza, A. Galli, P. Lampariello, G. Lovat, and S. Paulotto, "Modal properties of surface and leaky waves propagating at arbitrary angles along a metal strip grating on a grounded slab", *IEEE Transactions on Antennas and Propagation*, vol. 53, pp. 36-46, Jan. 2005
- P. Baccarelli, P. Burghignoli, G. Lovat, and S. Paulotto, "A novel printed leaky-wave 'Bull-Eye' antenna with suppressed surface-wave excitation", *Digest 2004 IEEE AP-S International Symposium on Antennas and Propagation*, Monterey, California, 20-25 June 2004, pp. 1078-1081
- P. Baccarelli, S. Paulotto, D. R. Jackson, and A. A. Oliner, "Analysis of Printed Periodic Structures on a Grounded Substrate: A New Brillouin Dispersion Diagram", accepted for presentation to *IEEE MTT-S International Microwave Symposium*, Long Beach, CA, June 11-17, 2005
- P. Baccarelli, C. Di Nallo, S. Paulotto, and D. R. Jackson, "A full-wave numerical approach for accurate modal analysis of arbitrarily periodic microstrip lines," submitted to *IEEE Transactions on Microwave Theory and Techniques*